Biomimetic Vascular Networks for Self-Healing Concrete

by David Heywood (SID)
Group D 2014/2015

Technical Abstract

Concrete dominates mankind's infrastructure and is the second most widely consumed material in the world (after water). The production of concrete is environmentally costly. Manufacture of cement, a key constituent of concrete, accounts for 7% of the world's carbon dioxide emissions. As a result any method by which we can improve the life and sustainability of our concrete structures is likely to have a profound, global effect.

Concrete is quasi-brittle, being strong in compression yet weak in tension. As a result areas of concrete loaded in tension usually contain reinforcement to support tensile loads where the surrounding material cannot. Despite this reinforcement, the formation of microcracks is seen as an inherent feature of this material. These cracks endanger the durability of the concrete as they allow the ingress of aggressive substances into the material matrix. If these substances penetrate deep enough to commence corrosion of the reinforcement catastrophic collapse of the structure may occur. As a result concrete structures require significant maintenance and repair equating to 45% of the UK's construction costs.

In order to solve the sustainability and economic problems associated with concrete structures the field of self-healing in cementitious materials has emerged. Almost all biological materials have the ability to heal themselves autonomically, often containing a multifunctional vascular network to deliver the constituents of healing to the damage site. Here the use of vascular networks and a circulatory system is investigated as a method of self-healing within concrete.

A thorough literature review is presented detailing current research within the field of self-healing materials with a particular focus on the use of interconnected networks and current methods proposed for self-healing concrete. It was found that little work has been undertaken related to the use of interconnected networks within concrete. However some successful results have been attained in polymer composites suggesting that this is a valid line of investigation and may represent a good opportunity for self-healing in concrete. Design criteria for a self-healing system within concrete were also identified for use in devising the system and assessing its success at the end of the process.

Networks were manufactured from polylactic acid (PLA) using a 3D printer and embedded within mortar specimens reinforced with mild steel wire. Healing

agent was circulated through the networks using a peristaltic pump. A colloidal silica healing agent was used due to safety concerns with alternative glue options that posed a hazard when pressurised within the system. Specimens were loaded in three-point bending to the point where cracking occurred, rupturing the embedded networks and releasing healing agent into the crack. The specimens were then submerged in a water bath to heal.

Initial testing showed that embedded networks did not reliably fracture in the same location as the surrounding matrix. Therefore an investigation was undertaken to investigate the use of a different print material that would reliably rupture at the cracking site. Results showed acrylonitrile butadiene styrene (ABS) was a more suitable material, due to its increased brittleness, for network construction and so this material was used in subsequent testing.

Network design was varied and found to have an effect on the recovery of both mechanical and durability properties. Specimens with more delivery tubes at the crack plane allowed for more complete healing agent coverage of the crack face. Maximum crack face coverage of 63% was achieved in specimens with three horizontal healing agent delivery tubes. An increase in crack face coverage was found to positively correlate with the recovery of specimen properties.

The durability recovery of healed specimens was tested via microscopy and sorptivity testing. Using microscopy, cracks were observed to be 96% obscured after 10 days of healing and all fully obscured after 28 days of healing. Results from sorptivity experimentation demonstrated good durability recovery of healed specimens. Healed specimens had a sorptivity of 159% of the sorptivity of an uncracked control whilst the equivalent value for cracked controls was 401%.

A maximum load recovery of 31% and stiffness recovery of 47% was achieved after 28 days healing. These results were low due to the properties of the colloidal silica healing agent and therefore subsequent studies in this area should aim to improve these values, possibly through the use of different healing agents such as cyanoacrylates or epoxy resins.

Healing over multiple cycles was not tested as, in the majority of cases, healing agent solidified within the network before a second damage event could occur (after 28 days healing). Different circulation regimes during the healing cycle may solve this problem in future.

The vascular networks designed and manufactured within this project have shown promise for self-healing in cementitious materials. In the short term further work is required to produce reliable and effective healing within these networks. Looking to the future, traditional concrete structures could become a thing of the past with new, sustainable, intelligent structures coming to dominate our built environment.

Contents

1 Introduction

1.1 Motivation

Mankind has been using concrete in pioneering architectural feats for millennia. The Romans used concrete-like materials widely, even creating an unreinforced 43.3 metre diameter concrete dome to top the Pantheon in Rome [1].

Modern concrete structures have been built since the discovery of Portland cement in the middle of the nineteenth century [2]. Civil infrastructure in today's world is dominated by concrete and it is the world's most widely used man-made material with over 1 cubic metre per person produced annually [3].

Cementitious materials are quasi-brittle, strong in compression whilst relatively weak in tension. As a result any areas of concrete loaded in tension usually contain reinforcement to carry tensile loads where concrete cannot.

The formation of microcracks is considered an inherent feature of reinforced concrete and they do not initially present a hazard to the structure. These microcracks may be formed via shrinkage, expansion, loading or creep [4]. However, if cracks become too wide or form an interconnected network, when combined with the inherent microporosity of concrete, then the capacity of the surrounding concrete matrix to protect the steel reinforcement from corrosive substances is significantly diminished. This represents a major problem as corrosion of steel reinforcement is the primary reason for the catastrophic failure of concrete structures.

1.1.1 Economic and environmental considerations

The microcracking of concrete is the primary cause of the need for maintenance and repair of existing structures. Civil infrastructure deterioration is becoming an ever-increasing problem in developed countries such as the United Kingdom, Germany and the USA. Repair and maintenance costs of existing structures accounts for around 45% of the expenditure of the UK's construction industry [5]. The annual economic impact of maintaining, repairing and replacing deteriorating structures is estimated to be $18 – 21 billion in the USA alone. Furthermore, repairs to concrete structures are often short-lived with over half of all repairs failing and requiring further repairs within a short time period [6].

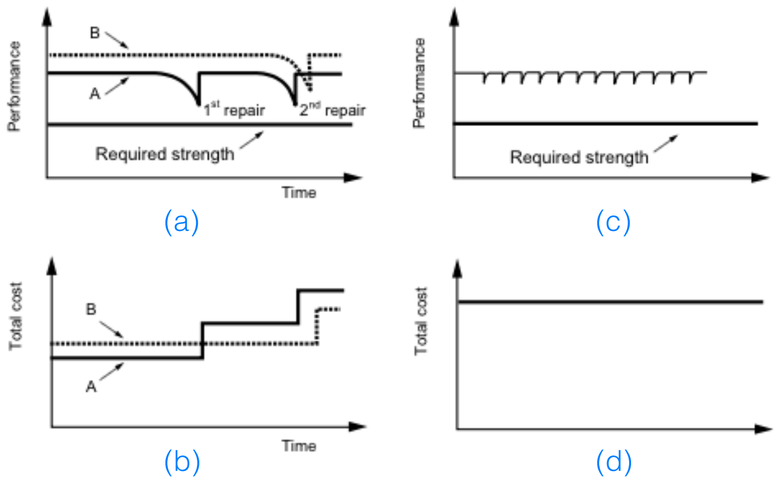

Figure 1: Graphs showing the economic advantages of self-healing structures (taken from [2]). (a) & (b) – The evolution of performance and cost with time elapsed for normal ('A') and high quality ('B') structures. (c) & (d) – The evolution of performance and cost for structures made from self-healing material.

Figure 1 graphically shows the economic motivation behind the design and utilisation of self-healing structures. An ideal self-healing structure, as displayed in Figure 1d, is one in which the initial cost of the structure equals the lifetime cost of the structure. It can be seen that costs of traditional structures increase over time as repairs are required. Although this model is simplistic and does not take into account effects associated with interest and inflation it clearly shows that increased initial investment in a self-healing structure may well result in reduced lifetime costs. Figure 1 also shows that if the self-healing mechanism is sufficiently easily triggered then the margin of safety of the structure (the difference between the buildings actual strength and its required strength) remains higher and thus the probability of a catastrophic failure is reduced.

Therefore the use of self-healing materials could represent a significant financial saving if the life of the building is sufficiently long.

Self-healing structures represent an opportunity to make infrastructure more environmentally friendly. A study by DEFRA found that the building and construction industry in the UK is responsible for up to 50% of the country's total CO_2 emissions [7]. Concrete is produced on such a vast scale globally that this process has a profound effect on global CO_2 emissions. The CO_2 production associated with the production of Portland cement (the dominant binder used in concrete production) is estimated at 5-7% of total global CO_2 emissions [2].

As countries such as India and China continue to expand the global demand for concrete, and hence the global CO_2 emissions associated with its production, is set to increase. The total global production of concrete is predicted to quadruple its 1990 value by 2050 [1].

An enhancement of the longevity of our built infrastructure and reduction in required repair and maintenance activities will undoubtedly reduce our environmental impact on the planet. As a result there is a clear motivation for the investigation of self-healing concrete from an environmental standpoint.

1.2 Aims and Objectives

This project aims to build on current research in investigating the use of biomimetic vascular networks (three dimensional hollow tubular arrays in which a healing agent is contained for transport to a damage site) for self-healing in concrete. The objectives of the project are as follows:

- To thoroughly review the current research and literature related to self-healing materials with a particular focus on self-healing concrete and the use of vascular networks for self-healing, thus identifying key areas for improvement and further research.

- To establish the requirements for the design of a vascular healing system within concrete.

- To design, manufacture and embed vascular networks within a cementitious matrix and successfully supply healing agent to a damage site.

- To investigate the quality of healing achieved, draw conclusions and identify areas for improvement and further investigation.

1.3 Report Outline

This report is divided into five distinct sections. Section 1, preceding this paragraph, introduces the motivation and aims for this project. Section 2 summarises literature and studies relevant to the project, identifying areas for improvement and further investigation. Section 3 describes the experimental method utilized within the project detailing the materials, equipment and methodology used as well as what each section of experimentation aimed to achieve. Section 4 lays out the results from experimentation and explores the consequence and significance of the findings. Section 5 summarises conclusions taken from the project and discusses directions for future research. At the end of this report references are listed and supplementary information is appended.

2 Literature Review

This section presents a summary of academic literature relevant to this project with key focus on work currently achieved and opportunities for further exploration.

2.1 Definitions for Self-Healing Materials

Multiple attempts to review current work and develop definitions in the emerging field of self-healing materials have been made. Several recent international collaborative efforts have aimed to consistently define terminology and lay a foundation for further research [4], [8]–[11]. This section details the conclusions of these efforts and defines terminology used throughout the report.

Current definitions for utilisation in the field of self-healing in concrete have been laid out by RILEM (The International Union of Laboratories and Experts in Construction Materials, Systems and Structures) [12], building on the work of the Japanese Concrete Institute (JCI) [13]. RILEM concisely defines self-healing as *"any process by the material itself involving the recovery and hence improvement of a performance after an earlier action that had reduced the performance of the material"* [12]. The design principles of self-healing materials are thus very different to those of traditional materials design.

2.1.1 Traditional and self-healing engineering materials design principles

Self-healing materials go against the grain of traditional materials design. Literature in this field makes a clear distinction between traditional engineering material design principles that aim to prevent damage from occurring and self-healing material design principles that aim to manage the damage as it occurs [8]. In the context of concrete, traditional design norms aim to delay the onset and progression of cracks into the material matrix. Eurocode 2, that specifies standards for concrete design, views cracking as an inevitability and sets a maximum crack width for serviceability of 0.25 mm [14]. Although this crack width does not damage the structural integrity of the member it does allow corrosive substances to enter the matrix. Over a number of years this represents a problem and hence self-healing methods to fill the cracks are desirable.

2.1.2 Autogenous and autonomic self-healing

As recommended by RILEM in a State-of-the-Art review self-healing can be divided into two distinct categories [12]. The first is that of *autogenic* healing in which the process of healing uses components that could otherwise be present in the material (without specific design for self-healing). Conversely *autonomic* healing describes processes in which components that would otherwise not be found in the material (engineering additions) are utilised in healing. These two categories encompass the entire field of self-healing materials.

These terms are especially relevant to concrete as cementitious materials have an autogenic ability to heal themselves. Autonomic self-healing within concrete has been the subject of considerable research in recent years with a wide variety of methods for autonomic self-healing having been established.

The repair of traditional concrete structures is a costly and time-consuming process that requires a large degree of intervention from human sources. Self-healing structures aim to limit the degree of human involvement required to maintain the structure at a serviceable level.

The trigger modes of self-healing materials may either be active or passive. Active release modes require some sort of human intervention in order to complete the healing process. Passive release modes are those in which no human intervention is required for the concrete to react to an external stimulus. The primary advantage of passive healing modes is that they, in theory, negate the need for human inspection, repair and maintenance. Active modes however are likely to inspire greater confidence in the end user as they allow a larger degree of control to be exercised.

2.1.3 Levels of material intelligence

Material intelligence describes the degree to which the self-healing process is controlled by the material. Figure 2 summarises the three main levels of material intelligence.

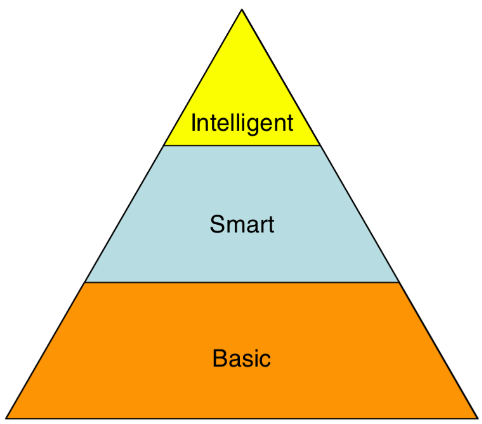

Figure 2: Hierarchy of material intelligence (taken from [12])

Basic materials contain the majority of engineering materials and are defined as those that have no response features. Smart materials are engineered materials that are able to exhibit a particular unique response in reaction to a change in the surrounding environment. In this the case the response of the material is said to vary linearly with stimulus strength. Intelligent materials occupy the pinnacle of this hierarchy. These materials exhibit a self-control capability whereby the material can gather, process and combine information to produce a particular controlled response. The majority of biological materials are classified as intelligent materials.

2.2 Self-Healing In Cementitious Materials

This section aims to briefly summarise the current methods of self-healing within the field of self-healing cementious materials to display the opportunities available and illustrate the advantages that vascular networks have to offer. As described above the self-healing mechanisms available for use within cementitious materials can be divided into two main categories: autogenic and autonomic self-healing.

2.2.1 Criteria for "robust" self-healing in concrete

When designing a self-healing system for use in a concrete structure a number of design criteria need to be considered. In order to set a clear aim for the design of self-healing concrete Li and Yang (2007) laid out a list of attributes that an ideal self-healing material should have in order to be considered as "robust" [15]:

- Pervasiveness: The healing mechanism should be ready for activation when and where damage (cracking) occurs.
- Stability: The healing mechanism should be ready for activation throughout the entire service life of the structure.
- Reliability: Healing must occur with a very low failure rate in a broad range of typical concrete structure environments.
- Quality: The properties of the structure should be returned to a level greater than or equal to pre-damage levels.
- Repeatability: The system should have the ability to repair multiple damage events.
- Economics: The material designed should be economically feasible given the highly cost sensitive nature of the construction industry.

2.2.2 Autogenic self-healing in cementitious materials

Autogenic self-healing within concrete is not a novel concept having been first noticed by the French Academy of Science in 1836 [16]. An engineer may play a role in the design of the material to optimise the mix and thus improve its natural self-healing mechanisms. As this type of healing is an innate quality of the material it is important to consider it when designing or testing any self-healing system for cementitious materials, as it will also affect the function of any autonomic healing processes. Figure 3 summarises the various causes of autogenic self-healing. As the figure shows the crack may be filled by physical, chemical or mechanical causes.

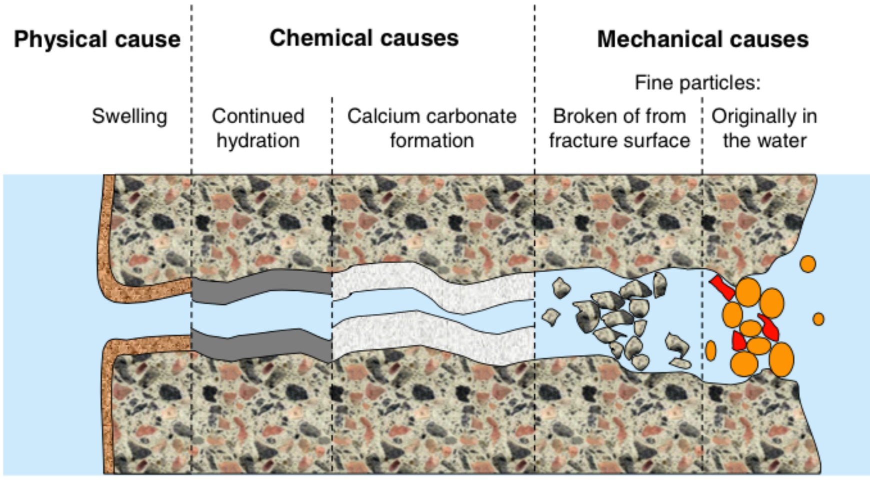

Figure 3: Summary of the various possible causes of autogenic healing within concrete (taken from [9]).

Of all these proposed causes it is believed that the crystallization of calcium carbonate is the primary mechanism of autogenic healing in practice [17]. The use of autogenic healing alone has two major disadvantages. First, the crack width must be small in order for the healing to be reliable. Maximum allowable crack widths of 0.01 – 0.3 mm have been established in various research, depending on environmental conditions and the specific composition of the mix [15]. The second major problem associated with this type of healing is that the quality of the healing is largely dictated by environmental factors that are outside of the designer's control. This method of self-healing does however have the advantage that it is relatively low cost and the minimal effort involved in altering the composition of the concrete mix.

2.2.3 Autonomic self-healing in cementitious materials

Autonomic systems for self-healing are the primary focus of current research. Wu et al. (2012) categorise the various methods of autonomic self-healing within cementitious materials into various key groups:

- Capsule based healing - In this method of healing static microcapsules containing a liquid healing agent are incorporated into the mix and designed to rupture as a crack propagates through the surrounding material matrix.

- Vascular healing - A network of hollow tubes, either internally encapsulated or connected to an external reservoir of healing agent, is contained within the material matrix. Cracking of the surrounding matrix causes cracking within the network and subsequent release of healing agent.

- Expansive agent and mineral admixtures - Expansive agent and mineral admixtures are incorporated into the mix and ideally generate expansive hydration products that fill cracks as damage occurs.

- Microbially induced carbonate precipitation - Bacterial spores are incorporated into the mix. Bacteria induced carbonate precipitation fills cracks in the cementitious material.

Autonomic healing methods aim to reduce the issues associated with autogenic self-healing detailed above. These different methods of autonomic self-healing all have associated advantages and disadvantages and there is currently disagreement within the academic community as to the best option (or combination of options) for self-healing within cementitious materials.

Research on microencapsulation is currently trying to solve the problem of manufacturing capsules that are sufficiently durable to survive the mixing process whilst also reliably cracking with the surrounding matrix (avoiding delamination between one half of the capsule and the crack plane) [18].

The main disadvantage of bacterial methods is that the high alkaline environment of concrete heavily hinders bacteria growth and therefore significant measures need to be taken to protect the bacteria [19], [20].

Microcapsules, expansive agent and mineral admixtures and bacterial spores have the advantage that they are easily incorporated into the mix during casting whilst vascular networks require careful installation and securing during the process. Although these networks may be relatively easily cast in small specimens a problem may occur when a large amount of concrete needs to be cast in an industrial application [21].

Stress concentrations in concrete structures are normally localised. As concrete structures fail by brittle fracture the crack will start from the largest flaw in the material in the vicinity of the location of the maximum tensile stress. Even if the initial crack is fully healed the general location of maximum stress in the structure will not change and hence a second healing event is likely to be required in the same location. Mechanisms of self-healing in which no transport of healing agent is available struggle to heal damage over multiple cycles as once the healing agent in one region is depleted it cannot be replenished. The dynamic delivery of healing agent allows for the fluid to be replenished after use in a particular damage event. Thus autonomic healing using vascular networks represents an attractive opportunity for recovery over multiple cycles and hence arguably the one of the best options to fulfill all of the requirements listed in 2.2.1.

2.3 Biomimetic Vascular Networks

Biomimetics is the imitation of the models, systems and elements of nature for the purpose of solving complex human problems. Vascular networks, as briefly described above, are hollow tubular structures designed to carry a functional fluid through a material matrix.

Over billions of years of evolution nature has developed materials that can self-heal. The majority of these materials contain a pervasive vascular network that supplies the necessary biochemical components for healing to occur. These networks are present in a wide range of organisms at different hierarchical length scales and are often fractal in nature (e.g the xylem and phloem of plants and the circulatory system of animals) [22].

Nature displays a huge diversity within the materials it uses. However care must be taken when using biological systems as a source of inspiration as they are optimised for more than one function. The functionality of an animal's circulatory system extends far beyond the delivery of clotting platelet cells to ruptured vessels. This natural vascular network also carries hormones, nutrients, gases, waste products, antibodies and white blood cells to fight disease and infection as well as helping to maintain homeostasis for every cell in the body. Thus the requirements of a biomimetic engineering solution, drawing inspiration from this system, should be carefully considered so as not to copy complexity required in the natural system for another functionality [23].

2.3.1 Tubular encapsulation of healing agent

Carolyn Dry was the first to propose the tubular encapsulation of healing agent for self-healing in concrete in the early 1990's [24]–[26]. Her experimentation used square prismatic beams enclosing an array of 16 brittle hollow glass fibres containing air-curing cyanoacrylate adhesive. Figure 4a shows a diagrammatic representation of her experimental setup. These specimens were loaded in three-point bending to the point where the glass pipettes were heard to have broken and then allowed to heal for 14 days before being retested to failure. Her results proved the viability of this passive method of self-healing as most of the loaded samples carried more load on the second bend (an average increase of 15%) than on the first whilst this was not the case for control samples. Samples in which healing agent had been released also exhibited greater toughness than control specimens. Dry also tested active modes of healing agent release yielding similar results. Hollow fibres were coated with wax so that healing agent would only be released from the fractured tubes when the concrete matrix was heated by an operator [25].

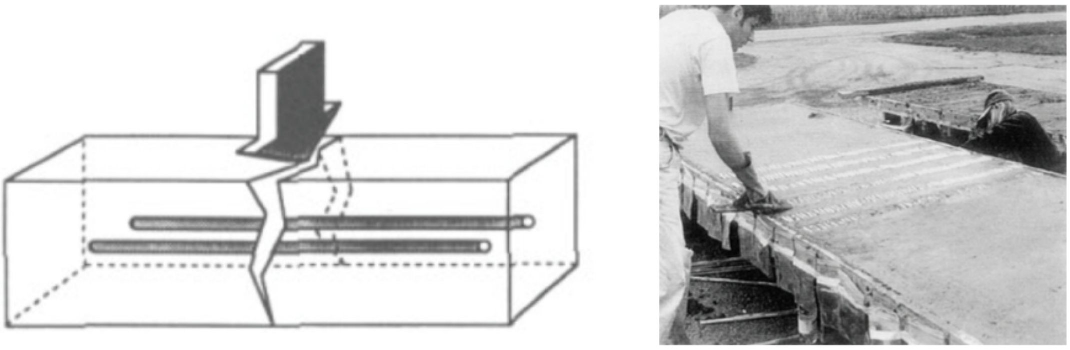

(a) (b)

Figure 4: Figures relating to Dry's experimentation. (a) Diagram of the basic experimental setup from Dry's initial experimentation (taken from [25]). (b) Photograph of tubes being embedded on the top surface of the bridge deck (taken from [52]).

In further experimentation Dry tested the viability of concrete specimens containing hollow tunnels coated with a brittle sealer [27]. The tunnels each contained one part of a three-part methyl-methacrylate adhesive system held separately from one another. Upon cracking the liquids leaked from the crack and combined filling it with a solid plexiglass-like matrix within 24 hours curing time. Again this research concluded that the adhesive bond created both restored the full strength of the sample and made the beam more flexible. This method of encapsulation, although advantageous in that the release of healing agent is immediate with the cracking of the surround matrix, is time consuming and costly to manufacture as hollow tunnels must be created by casting concrete around some removable former.

Following the success of earlier research Dry scaled up her experimentation to incorporate a self-healing system into structures on a usual civil application scale. 4 x 20 ft bridge deck slabs were cast containing hollow glass fibres (see Figure 4b). After a period of several months the slabs were then tested in three-point bending and the embedded glass tubes cracked releasing the healing agent. This experimentation was crucial as it demonstrated that this method of self-healing could occur after a prolonged period of time (thus meeting the 'stability' criteria detailed in 2.2.1) and was scalable to larger applications.

Further research has continued from Dry's work in this area and resulted in various different results and discoveries. Tran Diep Phuoc Thao et al. (2009) proposed the use of epoxy resin healing agent [28]. Using a similar experimental setup to Dry (casting mortar specimens containing glass tubes) they were able to demonstrate healing over multiple cycles. Specimens were loaded and broken in three-point bending, allowed to heal for 4 days and retested and then broken a final time after a further 3 days healing. During the second loading cycle (4 days) the specimen failed at a lower load than the virgin specimen (see Figure 5a). During the third loading cycle (7 days) the specimen failed at a load 32% higher than the failure load of the virgin specimen. The authors hypothesized that the lower failure load in the second loading cycle was due to insufficient air ingress into the crack tip during the first healing cycle resulting in the resin only curing at the crack mouth. The third crack was initiated in a new location (see Figure 5b) suggesting that the second crack had enabled complete healing of the original crack.

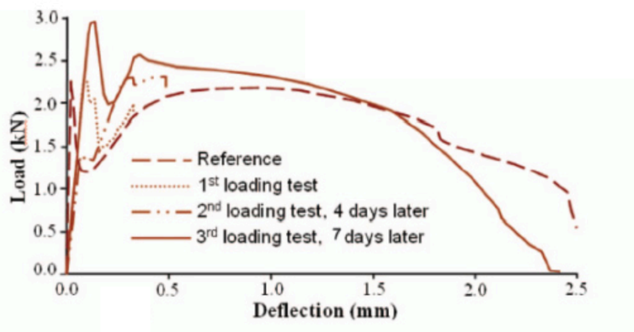

(a)

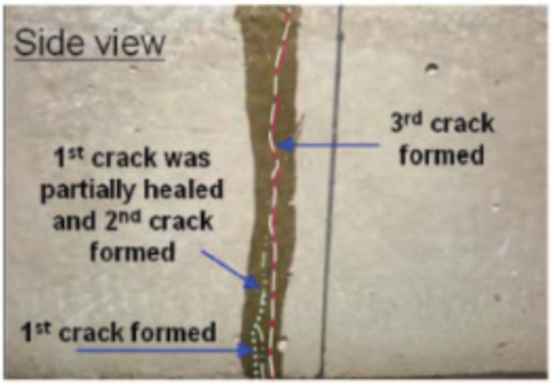

(b)

Figure 5: Experimental results from Thao et al. (2009) (both taken from [28]) (a) load deflection curve, (b) photograph showing the locations of crack formation.

These investigations were extended by Pang et al. to yield results for larger concrete structures as might be used in civil applications [29]. This involved the testing of glass tube healing systems encapsulated within 0.125 m x 0.2 m x 2 m beams, 0.2 m diameter x 0.8 m columns and 0.1 m x 1 m x 1 m slabs. All structures were loaded and unloaded over repeated cycles and self-healing efficacy was assessed by the stiffness recovery of the members. Beams, columns and slabs were tested in three-point bending, compression and dropped weight impact respectively. The beams recovered 84% of their initial stiffness, the columns up to 70% and the slabs up to 99%.

Further investigation into this type of encapsulation technique resulted in Joseph et al. (2010) discovering that healing agent release was significantly hindered by the negative pressure forces created at the far ends of sealed encapsulated tubes as the healing agent was released into the crack [30]. As a result a new type of healing system emerged in which tubes were in some way connected to the external environment.

2.3.2 Networks connected to the external environment

As a result of this discovery Joseph revised his experimental setup to that shown in Figure 6. In this setup 4 hollow capillary tubes, open to the atmosphere at either end, were filled with wicking grade, 5 cPs cyanoacrylate adhesive healing agent [30].

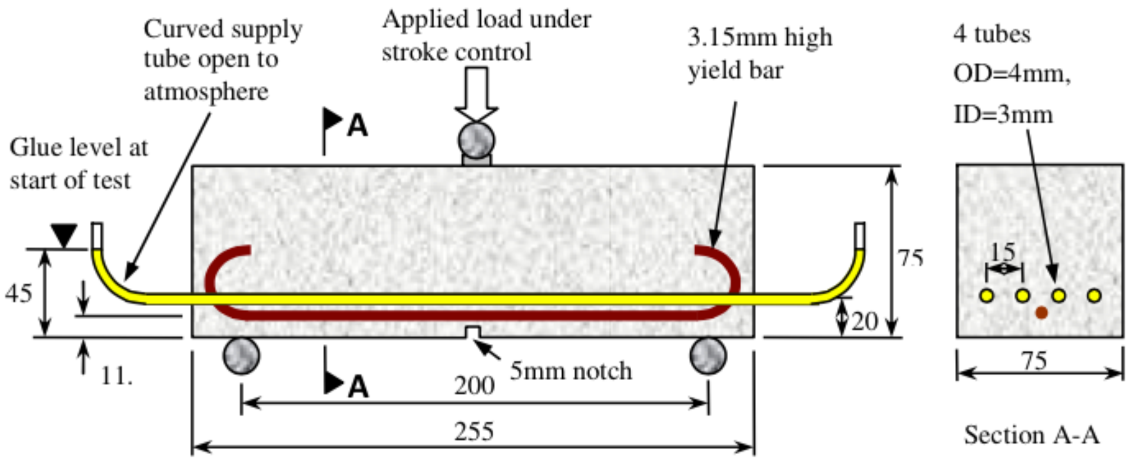

Figure 6: Joseph et al. revised experimental setup for three-point bending of specimens with tubes connected to the external environment (taken from [30]).

The specimens were loading in three-point bending to the point where healing agent release was observed. They were then unloaded and allowed to heal for 24 hours before being reloaded to failure. Results from the second round of loading showed that all samples exhibited increased stiffness, a higher failure load and a more ductile post peak response. As with the experimentation of Thao et al., Joseph's team observed that the new cracks formed in a different location to the primary crack suggesting that full healing of the crack had taken place.

A self-healing system's ability to release healing agent is of the utmost importance as the area covered by the healing agent dictates the quality of the healing achieved. In instances where a large volume of healing agent is required or where healing over multiple cycles has depleted internal healing agent supplies an external replenishment method is desirable. As a result studies have built on the concept of having the embedded network in some way connected to the external environment. Mihashi et al., for example, connected one end of embedded glass pipes to a 'repairing agent tank' elevated above the specimen thus applying a pressure to the healing agent within the internal tubes [21]. Dry and Corsaw investigated whether filling glass tubes with healing agent before or after cracking provided more reliable healing [31]. They concluded that it is better to provide an external reservoir with healing agent that is released after the crack appears. As a result, in further experimentation, a large volume of chemical was delivered by vacuum pressure that drew it through hollow glass capillaries contained within the specimen.

2.3.3 Healing agents for biomimetic vascular networks

Various studies have been carried out on the relative merits of different healing agents for self-healing in concrete [11]. Broadly speaking the healing agents tested may be split into three main categories: epoxy resins, cyanoacrylates and mineral compounds that can interact chemically with the cementitious matrix.

Epoxy resins are available in either one or two-part resins. One-part resins cure in the presence of heat whilst two part resins are cured when the hardener and resin components mix. One-part resins have had some success in previous experimentation [32]. Studies using two-part epoxy resin healing agents have often encountered problems due to insufficient mixing of the two components leading to poor bond strength [21].

Cyanoacrylates (superglues) are one-part healing agents that cure in the presence of moisture. Cyanoacrylates are acidic solutions and hence cure rapidly when they come into contact with concrete, which is an alkaline material ($pH > 12$). This fast curing may be advantageous for cyclical loading applications but also raises concerns that the healing agent may set before full crack penetration is achieved [11]. Cyanoacrylates have achieved good strength and stiffness recovery in previous studies [24],[33].

Mineral compounds such as sodium silicate (Na_2SiO_3) and colloidal silica (a fine suspension of amorphous SiO_2 particles in a liquid phase) react with calcium hydroxide in the crack faces to form calcium-silicate-hydrate (C-S-H). This has a healing effect as C-S-H is responsible for most of the good mechanical properties of concrete as it binds together cement particles into a cohesive whole.

The reaction that converts calcium hydroxide into C-S-H is slightly different for sodium silicate and colloidal silica. These reactions are as follows:

Sodium Silicate

$$Na_2SiO_3 + Ca(OH)_2 \xrightarrow{+H_2O} x(CaO \cdot SiO_2) \cdot H_2O + Na_2O \tag{1}$$

Colloidal Silica

$$SiO_2 + H_2O \rightarrow Si(OH)_4 \tag{2}$$

$$Si(OH)_4 + Ca(OH)_2 \xrightarrow{+H_2O} x(CaO \cdot SiO_2) \cdot H_2O \tag{3}$$

The sodium silicate reaction is more energetically favourable and hence sodium silicate provides slightly better recovery of mechanical properties. Despite this, both recover significantly less strength than the glues detailed above [21]. However, as a result of their healing mode, they cause less material compatibility problems than their glue based counterparts. Most importantly they represent far less of a hazard when pressurised in a vascular network as they are significantly less harmful than both glues mentioned above.

2.3.4 Vascular networks in other fields

In 2001 Scott White et al. published a paper on autonomic healing within polymer composites and since then the field of self-healing composites has attracted a lot of attention [34]. The use of vascular networks for self-healing materials has been investigated at various length scales within various different materials including bulk polymers [35] and polymer composites [36].

The field of self-healing structural polymers has expanded far quicker than its cementitious equivalent due to their broad range of applications in the aerospace sector. As a result significant research has been carried out into the use of microvascular networks for self-healing in polymeric materials.

The use of hollow glass fibres embedded in a composite laminate was pioneered by Bleay et al. [36] with further research in this area carried out by Pang and Bond in 2005 [37], [38]. Pang and Bond were able to achieve an average of 97% strength recovery using an epoxy resin healing agent in fibre-reinforced polymers.

The focus of research then shifted to the use of interconnected networks rather than discrete channel arrays (equivalent to the tubular encapsulation described above). Interconnected networks offer a distinct advantage in that they allow for healing agent to be supplied to a damage site over multiple damage cycles. By 2009 Kathleen Toohey and her team had achieved healing over multiple cycles using microvascular networks [39]–[41]. Figure 7 shows the designed networks for one and two-part healing agents. These networks were created by direct-write assembly via the extrusion of viscoelastic fugitive inks. The fugitive nature of these inks means that once a material is cast around them they can be liquefied leaving an interconnected network. Strength recovery of up to 100% was achieved. Two-part healing agent systems were shown to perform better, healing up to 16 consecutive damage cycles, than their one-part equivalents that were only able to heal up to 7 damage cycles.

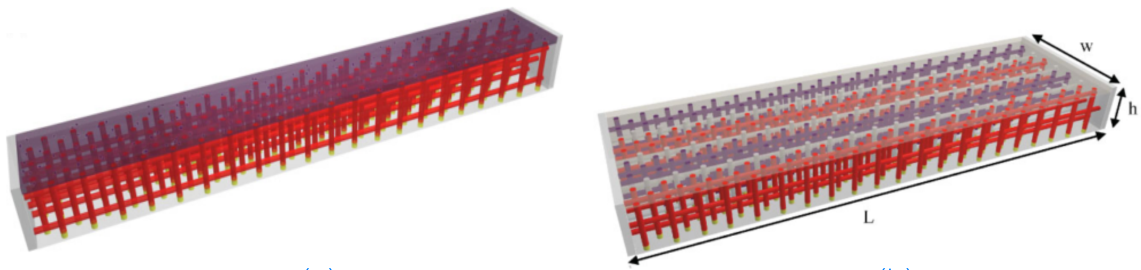

(a) (b)

Figure 7: Orthogonal microvascular networks (both from [41]). (a) Network for the delivery of a one-part healing agent to damage site. (b) Network for the delivery of a two-part healing agent, with different parts marked as red and blue tubes. Approximate dimensions of samples used are L = 42.5 mm, h = 8 mm, w = 12 mm.

2.4 Proposed Research

This project aims to utilize the research detailed above, linking the work of various authors and using the information gathered here as a foundation to ensure that the project is both relevant and original.

It is clear that work in the self-healing of cementitious materials currently lags behind the equivalent polymeric field and hence drawing lessons from Toohey's research may be of some benefit. However, because concrete contains aggregates far larger than the millimeter scale it is expected that the use of direct-writing techniques would prove unviable. Despite this, it is clear that the use of an interconnected network offers the best chance for healing over multiple cycles and current work in concrete has yet to fully take advantage of this finding.

This project aims to explore the opportunity presented. This is by no means a trivial challenge with the above literature review highlighting some key issues that need to be addressed:

- Any embedded vascular system needs to be brittle enough to crack in the same location as the surrounding concrete but tough enough to survive the casting process.

- The scalability of any experimental system should be considered throughout the process as the end goal is to design a system suitable for use in concrete structures.

- If an air curing healing agent is to be used then air ingress into the crack tip needs to be considered to achieve full healing.

- A method of securing the network within the system as well as a means of making the system pervasive needs to be considered.

Overall this literature review shows that significant progress in the field of self-healing concrete has been made over the last two decades. The potential to use biomimetic vascular networks in this field, and some of the associated challenges, are clear. The remainder of this report highlights how these challenges were addressed experimentally, the resulting findings and the conclusions that may be drawn.

3 Experimental Methodology

3.1 Design and Manufacture of the Vascular System

3.1.1 Network design

Effective network design is a crucial part to this project. Previous results showed that tubes of inner radius 4 mm and outer radius 5 mm represented the most effective geometry (avoiding manufacturing errors whilst being small enough so as not to significantly affect the mechanical properties of the specimen) [42].

Various network designs were considered. A few of the different designs evaluated may be seen in Figure 8. Figure 8a shows an orthogonal 3D interconnected network much like those seen in the work on self-healing polymers by Toohey et al. [41]. This design was discarded due to the fact that the networks would be very difficult to manufacture using the 3D printing method available as the printer can only print a layer in an area where one has already been deposited. In addition, their large volume would significantly reduce the mechanical integrity of any concrete structure.

Figure 8b shows a simple interconnected network and Figure 8c shows a more complex network with tubes of varying diameter better mimicking the vascular networks observable in nature. After much consideration a structure similar to that seen in Figure 8b was chosen. It was decided that the networks should be constructed as individual sections as may seen in Figure 9. This was to limit the complexity of parts and therefore reduce the chance of a printing error (3D printing, discussed shortly, was used to manufacture the networks). This modular method has the advantage that it keeps the individual components simple whilst being able to create relatively complex geometries.

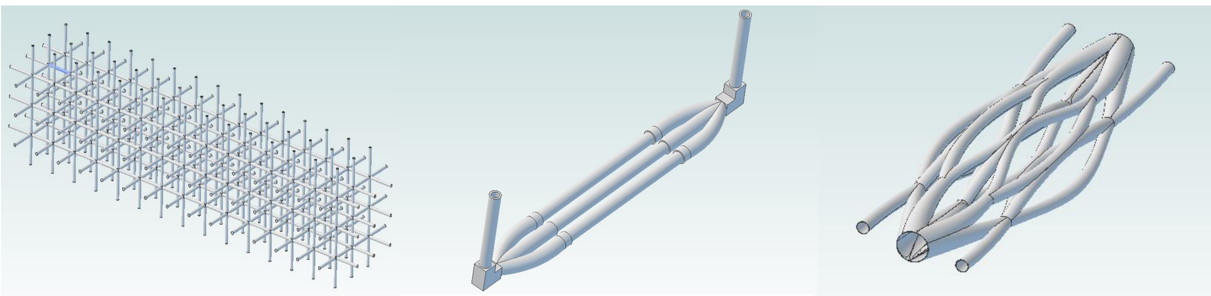

(a) (b) (c)

Figure 8: Different concepts for vascular networks. (a) An orthogonal array based on [41]. (b) A simple interconnected network made from constituent parts. (c) A vascular system with interconnected tubes of varying diameter, mimicking blood vessels (adapted from [42]).

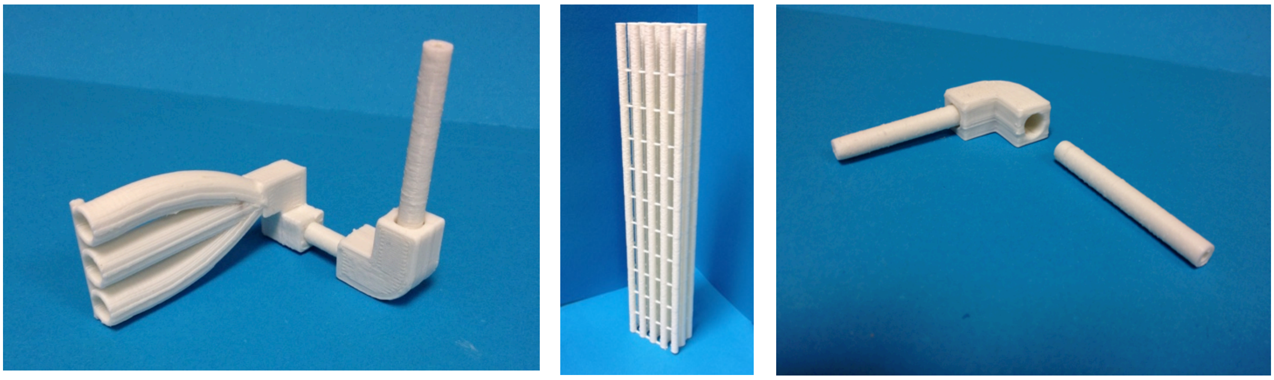

(a) (b) (c)

Figure 9: Photographs of network components. (a) A three-way divider designed to split the flow into three different tubes. (b) A group of 3D printed tubes – printed in a group to avoid printing errors. (c) Networks were made up of constituent parts.

If this method of self-healing were to be scaled up for use in industry it could be feasible that a 'plumbers-toolkit' of network components could be designed and subsequently assembled around the reinforcement. This method is likely to be more viable than the printing of large network components specifically optimised to the concrete structure's geometry.

Various network layouts were designed for experimentation. These networks either contained one, two or three horizontal tubes as seen in Figure 10.

3.1.2 Network manufacture and construction

The vascular networks used in this project were constructed using three-dimensional printing. This is an additive manufacturing technique in which successive layers of print material are deposited on top of one another in order to create a 3D object.

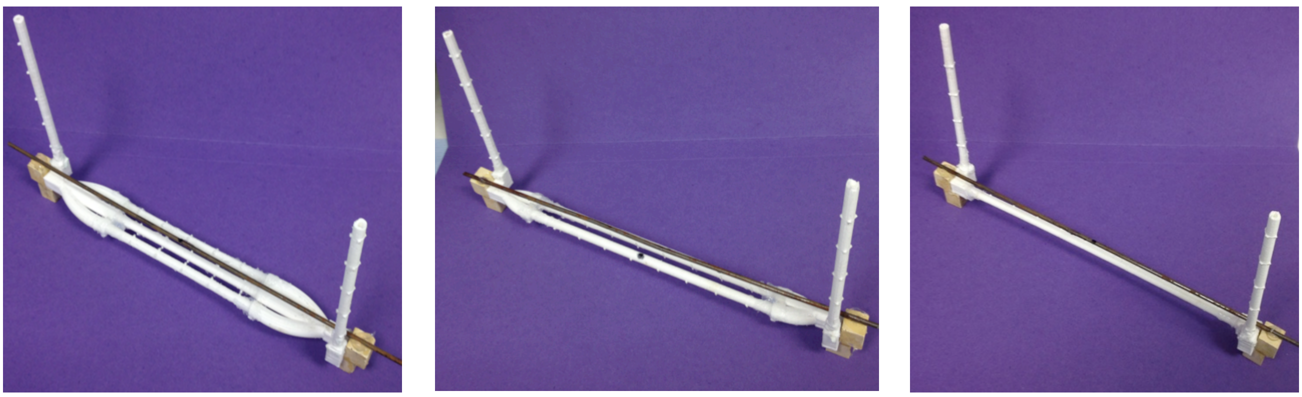

(a) (b) (c)

Figure 10: Figures showing the layout of the three different network types. (a) Network with three healing agent delivery tubes. (b) Network with two healing agent delivery tubes. (c) Network with one healing agent delivery tube.

This project used a CubeX™ 3D printer and associated software. Networks were designed on a computer using a 3D modelling software, Cubify® Invent™. These files were then converted to a print file using CubeX™ compiling software through successive slicing along the z-axis of the model. The resulting layered print file was then transferred to the printer and used to direct the print head as to where to deposit a material layer of constant thickness in the x-y plane. Once a layer has been deposited the print bed moves down a distance equal to the material layer thickness and the next layer is deposited. Thus a three-dimensional object is built up over time.

The single headed CubeX™ printer can produce a maximum part size of 275 mm (x) x 265 mm (y) x 240 mm (z) to tolerances of $\pm$1% [43]. The print layer thickness can be set to 0.1 mm, 0.25 mm or 0.5 mm. For the purpose of this project 0.25 mm thick print layers were used in order to allow for good part accuracy and reasonable printing times. The CubeX printer can produce printed parts in either Polylactic Acid (PLA) or Acrylonitrile Butadiene Styrene (ABS). The network was 3D printed in separate parts and glued together using cyanoacrylate adhesive.

3.1.3 Circulatory system and healing agent

It was decided through initial consideration and calculations that the network should be part of a circulatory system. There has be very little exploration of this method in prior research although it draws on the concept of interconnected networks experimented on in various studies [39]–[41]. This method allows the functional fluid to flow throughout the network and deliver healing agent to the damage site during multiple damage events.

The overall layout may be seen in Figure 11. The inflow pipe of the embedded network was attached, via rubber tubing, to a peristaltic pump that pumped healing agent from a reservoir of healing agent. The outflow of the network was piped back into the reservoir by another section of rubber tubing thus creating a complete circulatory system. The peristaltic pump circulated the fluid around the network at a volumetric flow rate of 60 ml/min.

Colloidal silica healing agent was used throughout this experimentation. The use of a pressurised system excluded the use of glues (such as those described in Section 2.3.3) for safety reasons. In control samples the networks were left empty throughout the test with no fluid circulated.

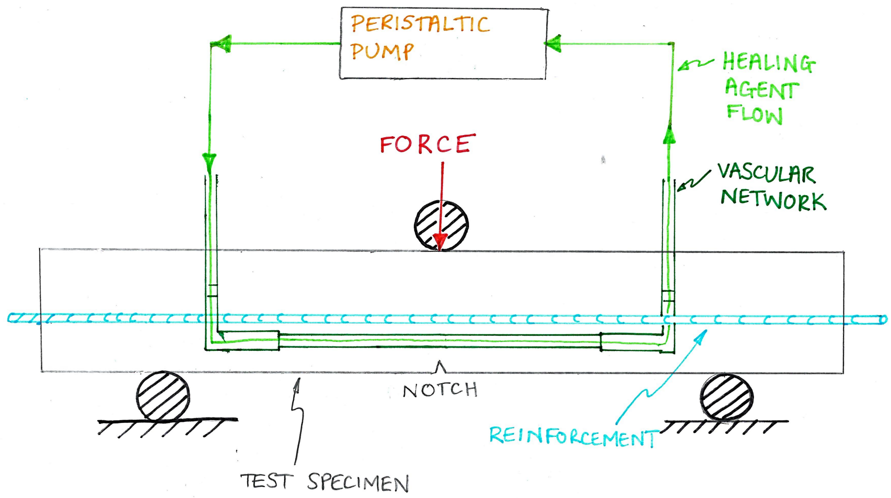

Figure 11: Schematic showing the basic concept of the proposed healing system; healing agent is circulated by a peristaltic pump.

3.2 Mixing and Casting

Square prismatic specimens were chosen as the primary method of testing the viability of embedded vascular networks in keeping with previous research within this field [24], [30], [42].

A mortar mix was utilised throughout this project as the small specimen size and intricate embedded networks inhibited the use of large aggregates. The mortar mix comprised of sand (maximum particle size 2mm), tap water and Ordinary Portland Cement (PC) (CEM-I, 52.5). These constituents were combined in a ratio of 1: 1.5: 0.4 (cement: sand: water) by weight. This composition was used in order to ensure that the resulting mix was fluid enough to flow into the small spaces between the limbs of the embedded networks and the mould walls.

Initial testing took place in 100 mm x 100 mm x 500 mm prismatic moulds. These were used as it was thought they would provide good volume for experimentation with different tube configurations. It was established that this volume was more than sufficient and therefore subsequent testing used 80mm x 80mm x 300mm prismatic moulds in order to make the specimens easier to handle and minimise material wastage.

Single straight mild steel bars of 5 mm diameter were used as light reinforcement in the larger specimens. The smaller specimens used 2.7 mm diameter mild steel wire for reinforcement. The 2.7 mm diameter wire was cut in 330mm lengths and bent through 90° at either end to give 30mm of vertical wire at either end for anchorage. The reinforcement was positioned at the correct height within the specimen using ceramic spacers and glued in place using silicone adhesive.

Figure 12 shows a prepared network/reinforcement assembly and a typical setup of moulds ready for the mortar mix to be poured in.

(a) (b)

Figure 12: (a) The full assembly of network, reinforcement and ceramic spacers ready to be embedded. (b) Moulds ready for casting.

3.3 Example Procedure for Specimen Preparation

3.3.1 Mould and mortar preparation

Networks and reinforcement were positioned within the mould according to the specific requirements of each test. The ceramic mounting blocks were glued to the base of the mould using silicone adhesive. The internal faces of the moulds were then lightly oiled to ensure a clean removal of the specimen after material setting.

The constituent materials of the mortar were measured out individually and then the sand and cement were added to the mixer and allowed to mix for 1-2 minutes. The water was then slowly added over the next minute. The mix containing all the constituent parts was then left to mix for another 2 minutes to ensure that a fully homogeneous mixture was achieved.

3.3.2 Casting

The mortar mix was then poured into the moulds in four parts. After each part of the mix had been added the mould was transferred to a vibration table to remove the air bubbles formed in the pouring process. The moulds were held in place by hand and the vibration amplitude was set so that the moulds rattled lightly but were still easy to hold in place. More mortar mix was only added to the moulds when air bubbles stopped rising to the surface of the mortar within the mould.

3.3.3 Curing

The specimens were allowed to set within the moulds for 24 hours before they were carefully demoulded and labelled. They were then transferred to a water bath to cure for 7 days and removed. After drying for a further 24 hours all specimens were notched to a depth of 3 mm across the base of the specimen using a rotating diamond blade cutter. The specimens were then tested.

3.4 Full Details of Specimen Layout

Preliminary investigations were carried out on five 100 mm x 100 mm x 500 mm mortar specimens with embedded three branch networks.

In order to test the effects of network layout on the reliability and quality of healing, three different networks were designed and embedded in 80 mm x 80 mm x 300 mm specimens. Figure 13 shows how the specimens were located within the specimens. Four specimens with each different network were cast resulting in twelve specimens in total.

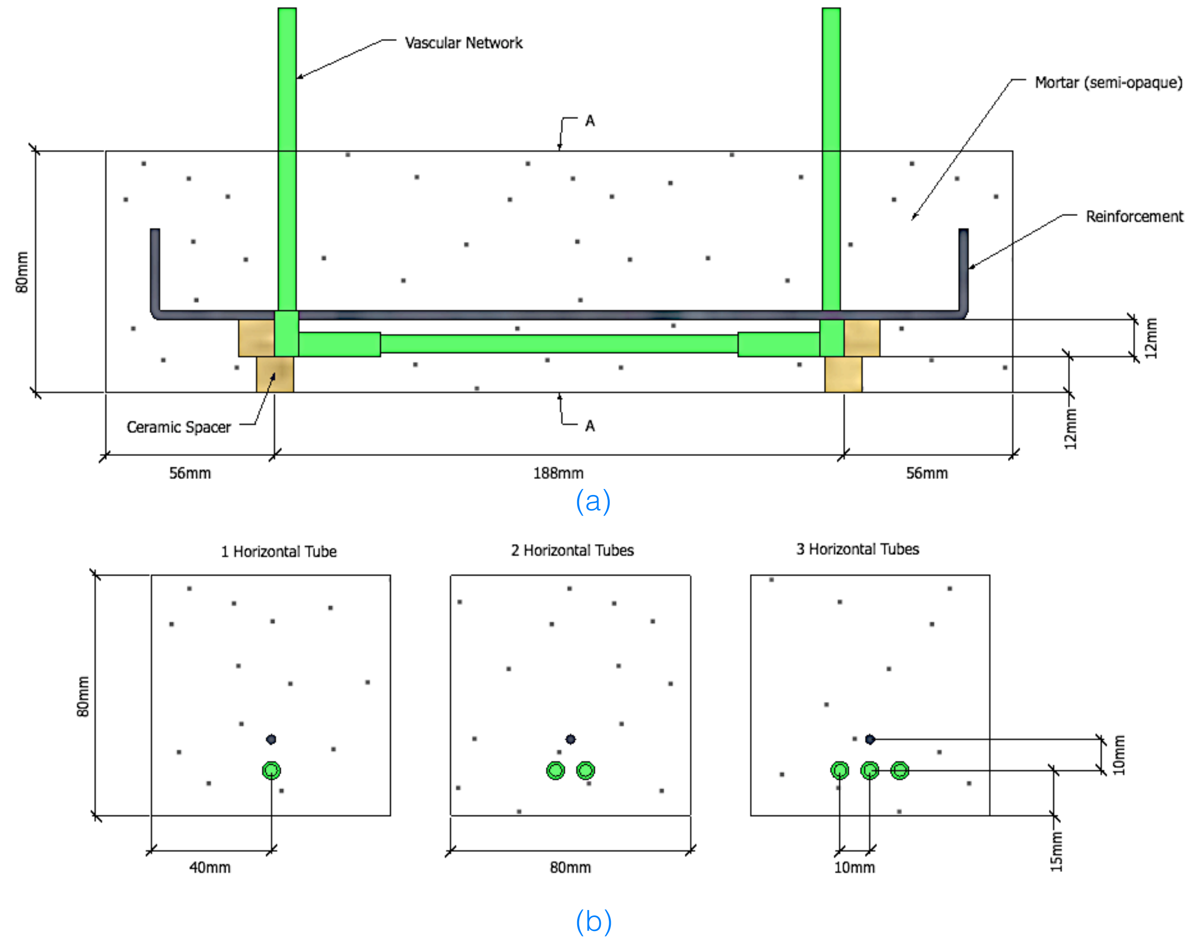

Figure 13: Schematics of the location of components within specimens. (a) Side view of a specimen showing the positioning of spacers, network (green) and reinforcement. (b) Section A-A for the three different network types showing one, two and three horizontal healing agent delivery tubes.

3.5 Experimental Methods for Testing Mechanical Property Recovery

3.5.1 Three-point bend testing

Specimens were cracked in three-point bending using an Instron® 5967 Dual Column Tabletop Universal Testing System with a 30kN load cell attached. The Instron® was set to record applied load and central deflection.

All specimens were initially cracked using the same loading regime. Samples were tested in three-point bending at a loading rate of 0.125 mm/min to the point where initial cracking occurred. The peristaltic pump was then turned on circulating healing agent through the network. The loading was stopped when healing agent leakage was observed. If leakage was not observed then specimens were loaded to a crack width of 1 mm and it was assumed an error had occurred and healing agent would not be released through the crack. 500 mm and 300 mm long specimens were mounted on supports 300 mm and 200 mm apart respectively. Figure 14 shows a photograph of a specimen undergoing three-point bend testing on the Instron® machine.

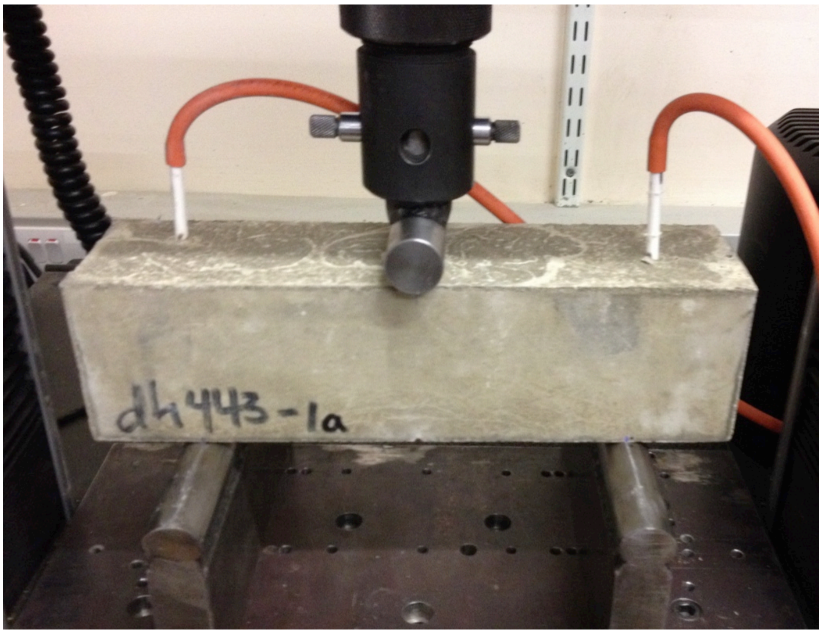

Figure 14: Photograph showing a specimen undergoing three-point bend testing. Orange rubber tubes attached to the white inflow and outflow pipes of the network.

In order to assess the recovery of the mechanical properties the specimens were reloaded to failure after 28 days healing. The peak load achieved before re-cracking was then recorded in order to calculate the load recovery of the specimen (expressed as a percentage of the initial peak load achieved in the first round of testing).

The load recovery percentage was calculated as followed:

$$\text{Load Recovery }(\%) = \frac{\text{Peak Load}_{28\text{ days}}}{\text{Peak Load}_{\text{Initial}}} \tag{4}$$

The values for stiffness recovery were calculated using simple beam theory. For a simply supported beam with a central point load the bending stiffness is given by:

$$\text{EI} = \frac{\text{WL}^3}{48\delta} \tag{5}$$

Where EI is the bending stiffness, W is the central load, L is the distance between supports and δ is the central displacement. The stiffness recovery for each beam was thus calculated by:

$$\text{Stiffness Recovery }(\%) = \frac{\left[{}^{\text{W}}\!/_{\delta}\right]_{28\text{ days}}}{\left[{}^{\text{W}}\!/_{\delta}\right]_{\text{Initial}}} \tag{6}$$

Where W/ δ was taken to be the average gradient of the load deflection curve in the linear region.

3.6 Experimental Methods for Testing Durability Recovery

3.6.1 Microscopy assessment of crack healing

An assessment of healing was carried out via examination of the reduction in crack area over time. After initial cracking photographs of the cracks were taken. This used a microscope and GXCapture software to photograph three points along the based of the specimen (see Figure 15) in order to measure reference crack areas and crack widths in the unloaded state. The specimens were then returned to the bath to heal for 28 days. In order to monitor the progression of the healing process the specimens were removed from the bath after 10 days healing and 21 days healing and allowed to dry for 4 hours. The cracks were then photographed in the same location using the method described above and returned to the bath to continue healing. After the full 28 days healing the specimens were then removed from the bath again and final photographs were taken of the cracks.

ImageJ image processing software was used to gather data from the photographs taken. This software allows the import of images with a reference scale, calibration of the software to millimeters per pixel and, as a result, measurement of lengths and areas enclosed by user-drawn shapes.

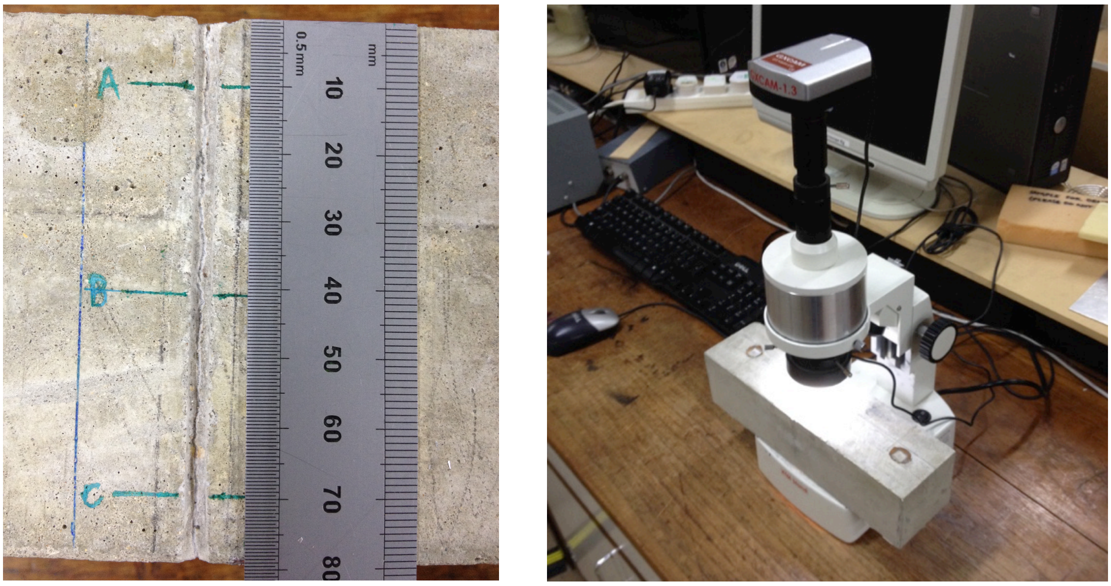

(a) (b)

Figure 15: Microscopy figures. (a) Photograph showing the three locations of crack where cracks were measured under the microscope, labelled A, B and C. (b) Photograph of the microscope and camera positioned over a specimen.

The software counts the number of pixels and then converts them into SI units. This was used to measure initial crack widths and measure the area of crack filled by the healing agent.

Photographs of the entire crack faces of the specimens were taken in order to assess the extent to which the healing agent had permeated the crack. Again ImageJ software was used to evaluate these areas.

3.6.2 Sorptivity testing

The term sorptivity is defined as a measure of the capacity of a medium to absorb and desorb liquid by capillarity. Sorptivity testing is a relatively simple parameter to determine and is increasingly being used as a measure of concrete resistance to exposure in aggressive environments [44].

Square prismatic specimens of 80 mm x 80 mm x 300 mm were cast. This number includes 15 specimens with triple branched networks embedded and 3 control specimens containing only the appropriate light reinforcement.

Initial cracking of specimens for sorptivity testing was carried out in three-point bending as described in Section 3.5.1. However instead of visual measurement of crack opening this method used a clip gauge. The clip gauge was attached to the base of the specimen (see Figure 16a). For this purpose small metal brackets were glued to the side of the specimen using a two-part epoxy resin. The clip gauge allowed to the maximum crack width to be held consistent (0.8 mm) across all specimens as dictated by the requirements of the sorptivity test.

Specimens were prepared for sorptivity testing by covering the lower face of the specimen with foil tape to stop water ingress into undesired areas (see Figure 16b).

(a) (b)

Figure 16: (a) Photograph showing the clip gauge mounted on clips glued either side of the specimen notch. (b) Photograph showing the foil tape applied to the base of the sample, leaving only a 10 mm wide strip around the crack clear.

A gap of 0.5 mm was left either side of the crack to allow for water to be drawn up into the crack by capillary action. Each sample's mass was measured initially with a mass balance to an accuracy of ±0.05 g. The specimens were then placed into a bath of distilled water so that the full base of the crack was just submerged. Figure 17 shows the experimental layout.

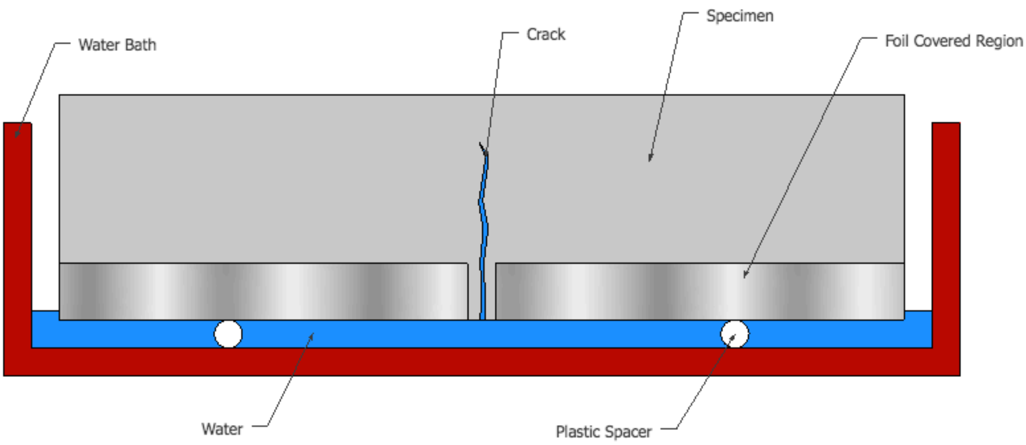

Figure 17: Diagram showing the experimental set up for sorptivity testing. The crack mouth is just submerged so the water is drawn up into the crack by capillary action.

At times $t = i\, minutes$ (where $i = n^2$ for $n = 1, 2, 3, \dots, 16$) the specimens were removed from the bath and excess water was wiped away. The specimens where then weighed, their mass recorded and then replaced in the bath. This allows the calculation of the mass of water absorbed by the area of specimen not covered by foil to be calculated. This is calculated as follows:

$$w(t) = m(t) - m_0 \tag{7}$$

Where $w(t)$ is the mass of water absorbed by the uncovered area at time t, $m(t)$ is the mass of the specimen at time t and m_0 is the initial mass of the specimen when dry. The absorption per unit area (g/m^2) for that suction period is then calculated by dividing $w(t)$ by the area of the uncovered surface. This value is then plotted against $\sqrt{t}$ and the gradient is the sorptivity of the specimen ((g/(m^{2}s$^{0.5}$)) as per RILEM TC 116-PCD [45].

4 Results and Discussion

4.1 Preliminary Testing

Preliminary testing was carried out in order to assess the viability of the designed network's self-healing in concrete. PLA was chosen as the material to construct the networks based on material selection carried out by Kimber (2014) [42].

Table 1 shows the circulation data for the first and second round of loading of 100 mm x 100 mm x 500 mm specimens. It can be seen that the fluid circulated through the network after casting in all but one specimen (specimen 2 in Table 1). This was due to the network in specimen 2 being damaged during the process of fixing it into the mould. This proved that the network manufacture and assembly methods could withstand the casting process for a simple mortar cast.

Table 1: Summary of the results from preliminary investigations

	Initial Cracking		Cracking After 28 Days Healing		
Specimen	Fluid circulates after casting	Fluid visible exiting crack during test	Fluid circulates after casting	Fluid visible exiting crack during test	Load recovered
Control	N/A	N/A	N/A	N/A	Minimal
1	Yes	Yes	Yes	Yes	30.60%
2	No	No	No	No	Minimal
3	Yes	Yes	No	No	Minimal
4	Yes	No	No	No	Minimal

Table 1 also shows that two of the functioning three networks leaked effectively upon the fracture of the specimen under loading allowing the healing agent to permeate the crack. This is an indication that the network fractured in the same location and at the same time as the surrounding matrix. Crack opening upon leakage was also recorded and found to be 0.7 mm for both of the two specimens.

After 28 days healing in the water bath the specimens were then retested and the results are summarized in Table 1. Of the three networks in which the fluid initially circulated only one remained unblocked after the curing process. This was due to the solidification of some of the healing agent within the network.

All five specimens cracked along the same fracture plane as before. This round of testing established that significant healing had not occurred in specimens where the healing agent was not released (as might be expected). Of the two specimens where the healing agent was released effectively only one showed significant strength recovery – it recovered 30.6% of its original failure load before failing.

Overall the results from this initial experimentation were very encouraging and proved the viability of this method for self-healing. These results showed that the method of network construction and manufacture is valid and sufficient to withstand the loading applied during casting. They also showed that it is possible to heal a crack and have the fluid still circulate through the network (and hence proved that healing multiple damage cycles should be possible using this type of arrangement). Nevertheless, it was decided that further measures should be taken in order to try and ensure that the fluid did not solidify in the tubes during healing.

Having learnt from this initial testing with a single layout of network an investigation into how the geometry of the embedded network affected the quality and reliability of healing was carried out. It was decided that subsequent testing should be carried out in smaller (80 mm x 80 mm x 300 mm) specimens for ease of experimentation and to reduce material wastage.

4.2 Testing Different Network Geometries

Three different network types (described in detail in Section 3.4) containing one, two or three healing agent delivery tubes were embedded within specimens in order to investigate the efficacy of healing associated with different network geometries. These networks were constructed from PLA.

4.2.1 Healing-agent release and recovery of mechanical properties

Table 2 summarises the strength and stiffness recovery of the specimens with different embedded networks. All values are listed as percentages of their original peak values obtained in the first round of loading. It is clear that low load recovery was achieved across all specimens whilst some stiffness was recovered. Again during the second loading cycle the majority of tubes were blocked by solidified healing agent (assumed to be silicic acid gel) and hence healing over multiple cycles could not be established.

Table 2: Summary of the results from testing the specimens on the Instron machine after 28 days healing in the water bath. Samples labeled *XT.Y* where *X* is the number of horizontal tubes and *Y* is the specimen number.

	Observed Fluid Leakage (Initial Cracking)	Observed Fluid Leakage (Second Loading Cycle)	Stiffness Recovery	Load Recovery
1T.1	No	No	29.5%	Minimal
1T.2	No	No	24.5%	Minimal
1T.3	No	No	30.1%	Minimal
1T.CONTROL	N/A	N/A	26.4%	Minimal
2T.1	Yes	No	45.3%	9.3%
2T.2	Yes	No	33.9%	6.9%
2T.3	Yes	Yes	35.9%	9.8%
2T.CONTROL	N/A	N/A	28.1%	Minimal
3T.1	Yes	Yes	46.6%	18.3%
3T.2	Yes	Yes	37.5%	13.7%
3T.3	Yes	No	46.4%	10.3%
3T.CONTROL	N/A	N/A	27.1%	Minimal

Although some autogenous healing may be anticipated in all samples it was not expected that this effect would be significant as the cracks were wider than 0.5 mm and hence this mode of healing is unlikely to have an effect over the healing time of 28 days. This is visible in Table 2 as none of the control samples recovered significant strength.

Although healing agent release was observed in all samples with two and three delivery tubes (see Figure 18a), the best strength recovery was observed in samples with three delivery tubes. This small load and stiffness recovery was expected as colloidal silica does not act as a glue bonding the two crack faces back together but reacts with calcium hydroxide at the crack faces to form C-S-H (as described in Section 2.3.3). Other measures of healing efficacy (i.e. crack closure and sorptivity) are investigated further in subsequent testing.

In all samples with one delivery tube (labeled 1T.Y in Table 2) no healing agent was released into the crack face. This was assumed to be due the embedded network tube cracking in a different location to the concrete (as had been hypothesized in the initial testing). After the second round of testing this was shown to be the case by inspection of the crack face (see Figure 18b). This result suggested that the network members were not brittle enough to undergo reliable fracture.

A number of useful conclusions and observations were obtained from this experimentation. Of greatest significance was that the three tube delivery system gave the best recovery. This may have been due to an increase in the area reached by the healing fluid and hence crack faces were analysed further to see how healing agent penetration across the crack faces varied with different geometries. It was found that the tubes often did not crack in the same location as the concrete

(a) (b)

Figure 18: (a) Visible healing agent release through the crack along the underside of a specimen. (b) Examination of the fracture plane confirming that healing agent was not released due to the network tube fracturing in a different location to the surrounding matrix.

specimen and thus an investigation into finding a more suitable network material than PLA was undertaken in order to solve this problem.

4.2.2 Pervasiveness of healing agent flow

Figure 19 shows pictures of the crack faces for different network configurations. The area covered by the healing agent is highlighted in each case showing the depth by which the healing agent penetrated the crack within this experimentation. Figure 19a shows the one delivery tube configuration in which no healing agent was released. The pattern observable on this crack face is due to the influx of water by capillary action during the 28 days healing (similar patterns were observed in control specimens). Examination of the all the samples showed that healing agent filled and average of 38% and 63% of the available crack area for the two and three delivery tube configurations respectively (Figure 19b and 19c). This difference in crack area covered by healing agent is likely to account of the difference in the strength recovery of the specimens observed in Table 2 (Section 4.2.1).

(a) (b) (c)

Figure 19: Crack face coverage pictures; yellow shaded region is area covered by healing agent. (a) One tube system in which no healing agent was released. (b) Two tube system. (c) Three tube system.

4.2.3 Visual analysis of healing with different network geometries

Specimens were removed from the bath at 10 and 20 days and the cracks were examined and photographed as described in Section 3.6.1. Figure 20a-c shows the progression of crack healing in a control specimen in which no healing agent was circulated. Figure 20d-f shows the progression of crack healing for an example specimen in which healing agent was circulated through the network and released into the crack. It may be seen from these figures that the crack was almost immediately filled with healing agent (visible in Figure 20d). The crack in this sample reduces in size slowly but is also clearly obstructed by crystals of the healing agent.

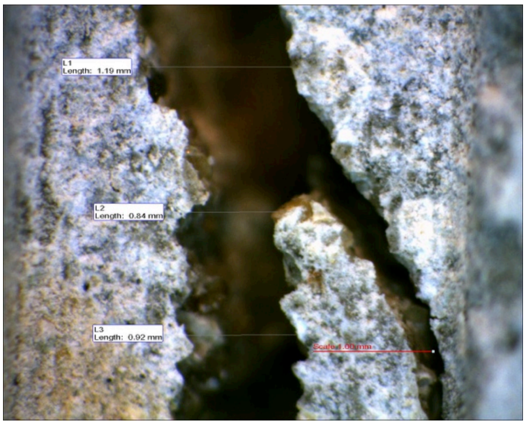

(a) - Control Specimen (10 days)

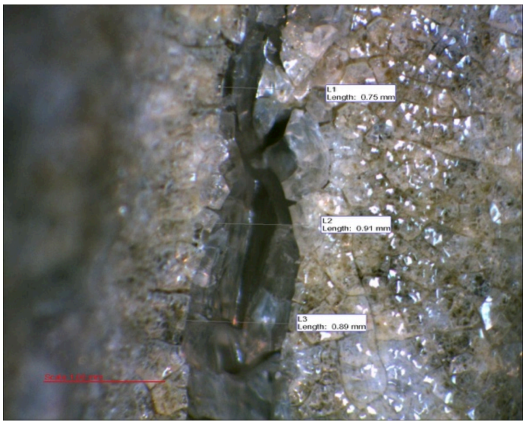

(d) - Healed Specimen (10 days)

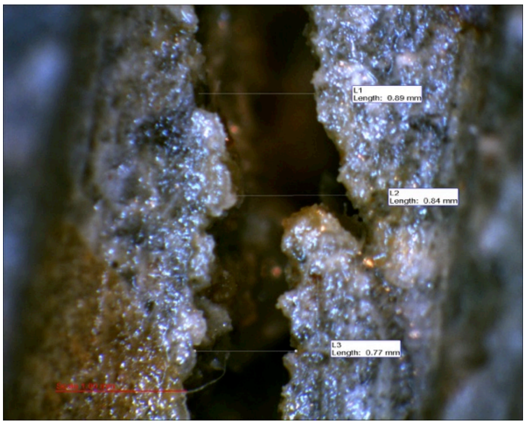

(b) - Control Specimen (20 days)

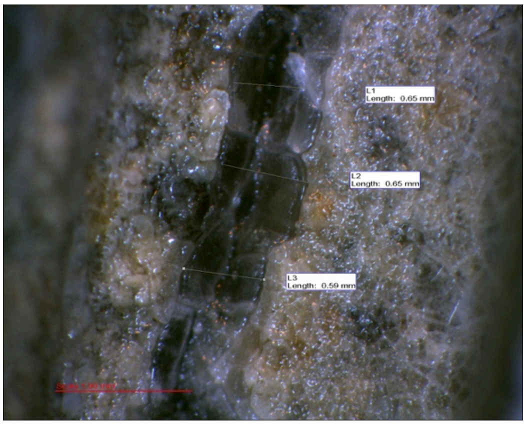

(e) - Healed Specimen (20 days)

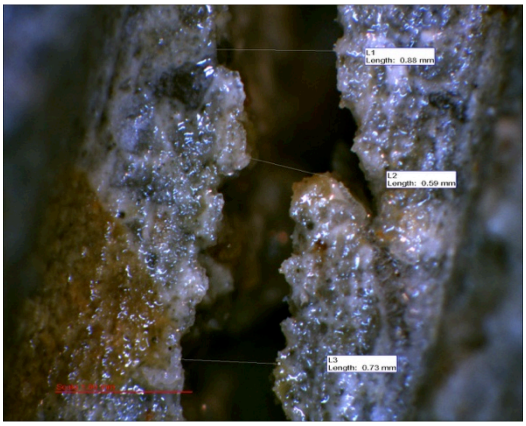

(c) - Control Specimen (28 days)

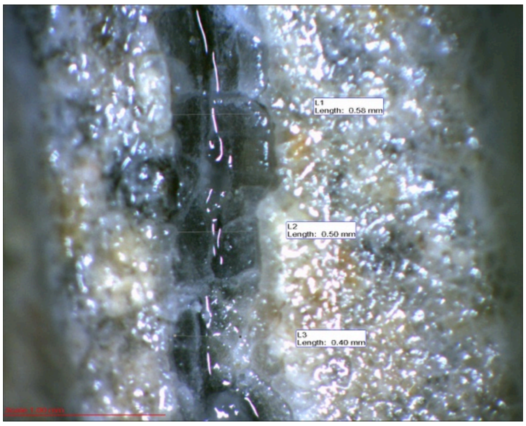

(f) – Healed Specimen (28 days)

Figure 20: Pictures showing the progression of crack healing for a control specimen (left hand side of page) and a healed specimen (right hand side of page).

The control sample, on the other hand, shows an empty crack. The autogenic healing process of concrete is clearly observable in these figures. The smaller crack to the left of the main crack is almost entirely filled in by autogenic healing after 20 days.

An average of the crack area reduction for each of the three measured locations (see Figure 15a in Section 3.6.1) on each sample was calculated. An average was taken across values for each different tube configuration for comparison between geometries (full results from this experimentation may be found in Appendix B). Figure 21 shows a graphical summary of these results.

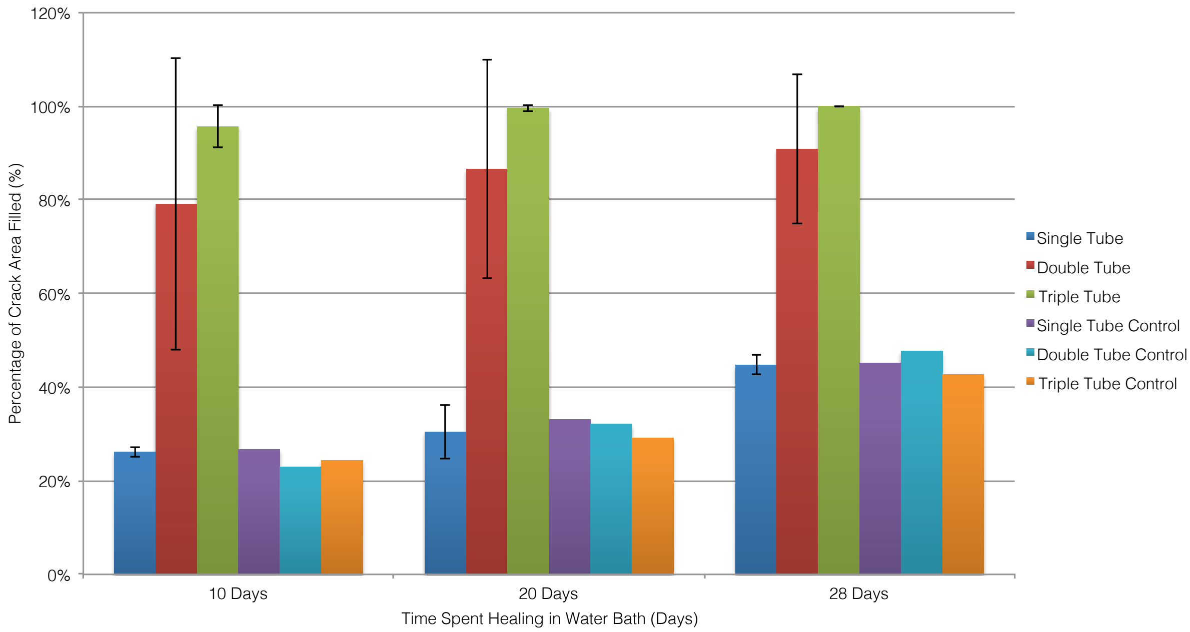

Figure 21: Summary of the results from inspection of crack healing at 10, 20 and 28 days. Error bars on healed specimens denote ± one standard deviation. (Insufficient data was collected to establish error bars for controls).

Figure 21 clearly shows that the healed samples had a far higher proportion of crack closure than those not subject to healing agent release. In the samples with one healing agent delivery tube there was no healing agent release and hence only a small reduction in the crack area (due to autogenic healing) was observed over the 28 day healing period. A similar trend may also be observed in the control samples in Figure 21. The consistency of results in samples in which healing agent was not released was good, with little variation between the three different control specimen types suggesting that the different network geometries have little effect on the autogenic healing process of the concrete.

Samples with two horizontal healing-agent delivery tubes (seen in red in Figure 21) showed substantially more of the crack filled over time than control samples. The error bars on the figure show a one standard deviation of the results above and below the mean value calculated. The large standard deviation in these results was caused by one reading showing considerably less reduction in crack area than the others (despite healing agent release). This result may be observed in Sample 2T.3 in Appendix B. It was decided this result should be included in the final dataset due to the small sample size as it may represent a statistically important observation in the two delivery tube geometry. Although the cause of this result was unclear it may have been due to one of the two tubes failing to fracture in the correct location hence reducing the area of the crack covered by released healing agent.

Cracks within specimens with three tubes were 96% obscured after 10 days. Figure 20d above shows an example in which the crack is almost fully obscured after 10 days. These results show that a three tube delivery method is the most reliable for healing agent delivery to the crack face.

From these results it is possible to conclude that an increase in the number of vessels present at the crack plane for fracture increases the quality of healing that takes place. If this method of self-healing were to be used in industrial applications then there would be a trade off between having a larger number of tubes present at the crack plane and the increase in cost and decrease in mechanical properties of the structure that this increase in tubes represents. Other factors will also affect the pervasiveness of the fluid through the crack such as the pressure of the fluid within the network. Further experimentation could explore the effect of pumping pressure on the healing agent coverage. A crack closure force could be applied to either end of the specimen forcing the two faces of the crack together and therefore improving the effectiveness of healing.

4.3 Testing Different Materials for Network Construction

Experimentation showed that networks manufactured from PLA did not consistently fracture in the same plane as the surrounding mortar matrix. Hence an investigation was carried out to identify a material that would fracture more consistently at the correct location.

As detailed in Section 3.1.2 the two materials available for use in conjunction with the CubeX™ 3D printer are ABS and PLA. PLA was initially chosen due to research conducted based upon the properties of the bulk material (observable in Table 3) [42]. Analysing this data it would appear that PLA was a better choice due to its higher stiffness and lower failure strain. However a brief analysis of parts printed from the two different materials was undertaken and suggested that parts printed from ABS may be more brittle than those printed in PLA.

Table 3: Summary of material properties for Acrylonitrile Butadiene Styrene (ABS) and Polylactic Acid (PLA) [53].

	PLA	ABS
Young's Modulus / GPa	3.5	1.9
Ultimate Tensile Stress / MPa	50	40
Density / g/cm^3	1.25	1.06
Typical Elongation at Break	6%	20%

In order to test this hypothesis, tubes (with nominal internal and external diameters of 4 mm and 5 mm respectively) were printed from both materials. These tubes were then tested individually on an Instron® machine in order to establish their response under loading. Table 4 summarises the results from this experimentation.

Table 4: Summary of results for testing of PLA and ABS 3D printed tubes

	PLA	ABS
Average Deflection at failure / mm	13.8	8.4
Average Load at failure / N	27.5	6.3
Effective Young's Modulus / GPa	2.6	1.1

Table 4 clearly shows that the ABS tubes failed at both a lower deflection (equilvalent to a lower strain) and a lower load than equivalent PLA tubes. Despite this fact the Young's moduli of the two materials were comparatively unchanged during the printing process. Figure 22 shows photographs of the layers that make up the individual tubes. The clear difference in the quality of the two microstructures is the likely reason for the large discrepancy in failure load and strain between the two tube types. The 3D printed layers within the PLA tube are far more uniform whereas layers in the ABS tube have large imperfections where the print head finishes one layer and moves on to the next. These imperfections between layers act like a crack within the material and make it far more brittle than a solid ABS tube. As a result, somewhat counterintuitively, the ABS tubes' lower manufacturing quality makes them a better option for use in parts of the network which are required to crack and release healing agent at the same time as the surrounding matrix.

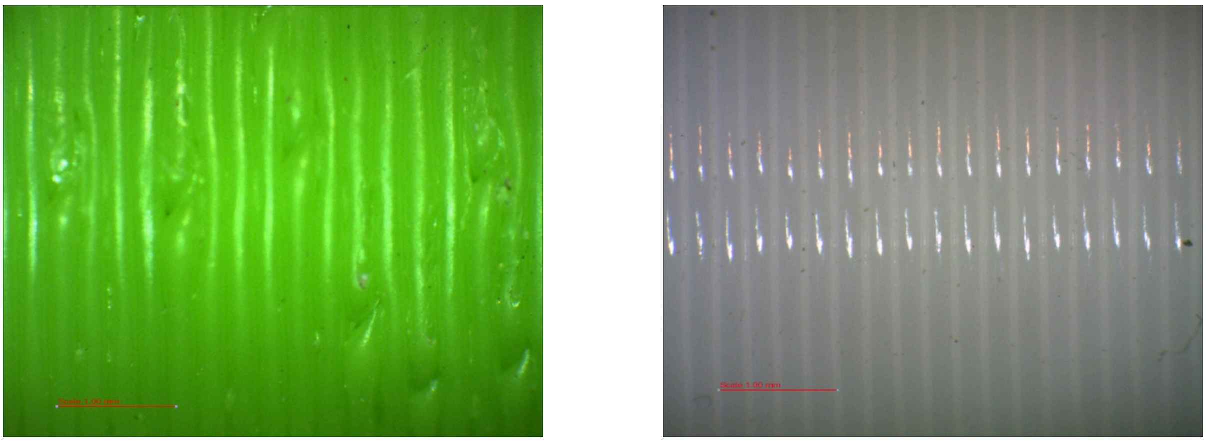

(a) (b)

Figure 22: (a) The layered microstructure of an ABS 3D printed tube showing non-uniform 0.25 mm layers and disjoins where the print head finishes one layer and moves onto the next. (b) The layered microstructure of a PLA 3D printed tube with uniform 0.25 mm layers.

As a result of this analysis the design of the networks used in subsequent experimentation was altered such that they contained ABS tubes in locations that were likely to crack under loading and PLA sections in other locations. This ensured the structures remained as durable as possible to withstand any damage that might occur during the casting process whilst cracking more readily in the desired location. Figure 23 shows an example of one of these networks with green ABS healing agent delivery tubes and white PLA inflow and outflow tubes.

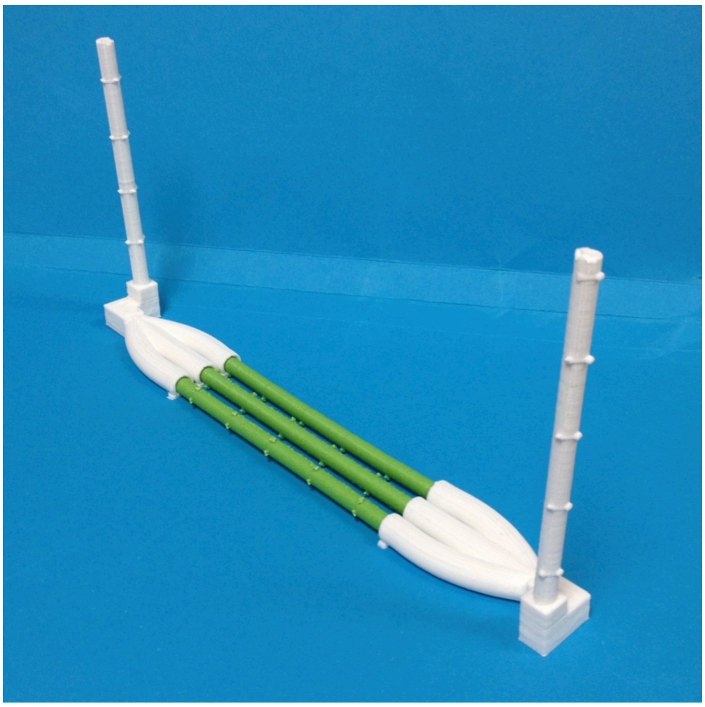

Figure 23: A vascular network made from ABS (green) in tubes likely to fracture under normal loading conditions and PLA (white) for network components supplying these fracture tubes.

4.4 Quantitative Analysis of Healing Efficacy over Time

As described in Section 3.6.2, the ability of concrete to absorb water through capillary action can have a profound effect on the durability of the material. As a result a full, quantitative investigation of the healing ability of the method of self-healing designed in this project requires an assessment of sorptivity. A lower sorptivity is desirable as it means that the concrete is less permeable to the ingress of water.

The mixed networks with ABS and PLA components shown in Figure 23 were used within this experimentation. Figure 24 summarises the results from this experimentation (a full table of results may be found in Appendix B).

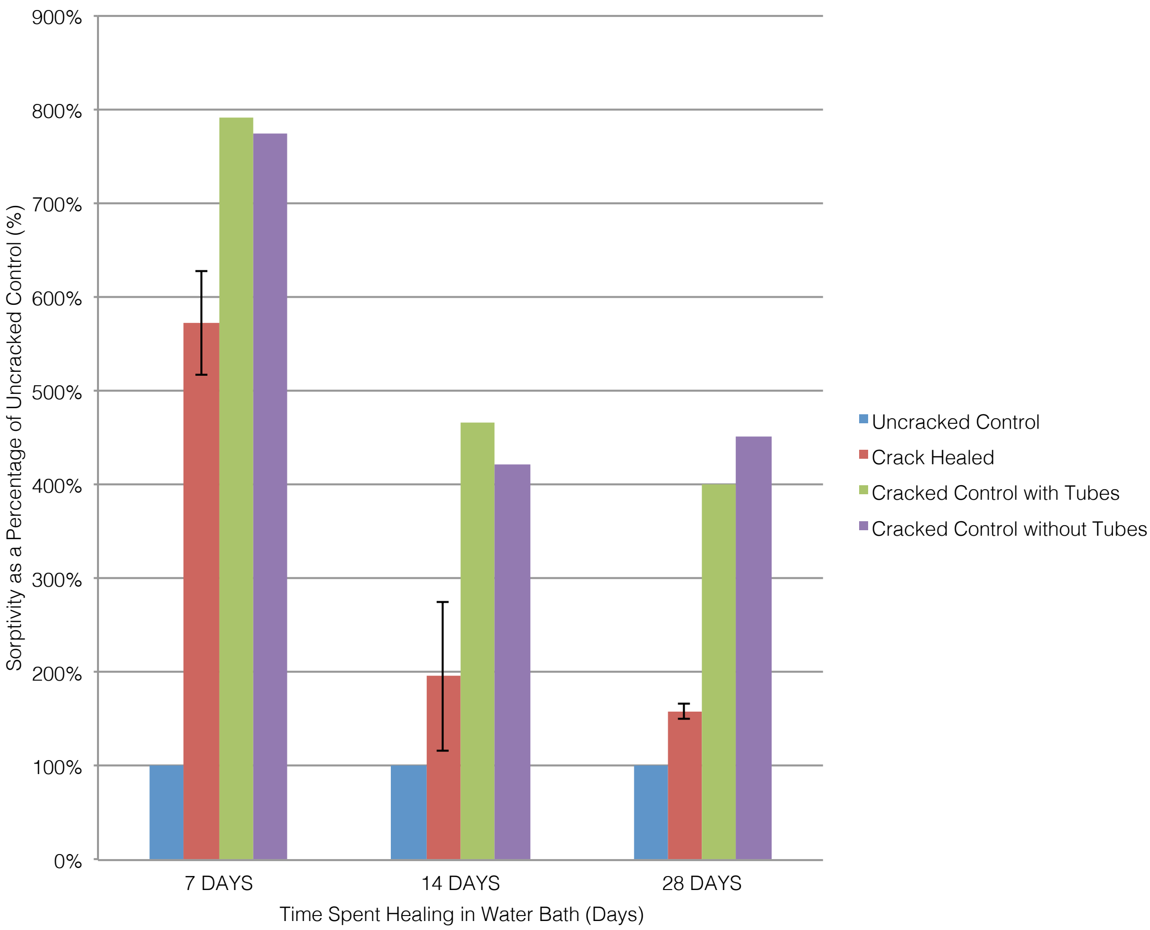

Figure 24: Summary of the results from sorptivity experimentation. All sorptivity values are listed as percentages of the sorptivity of an uncracked control specimen exposed to the same environmental conditions.

All values listed in Figure 24 are listed as percentages of the sorptivity of an uncracked control sample at each time period (shown in blue). It is clear from this figure that samples in which healing agent was released show lower sorptivities than equivalent controls. Further to this the healing process is accelerated by the presence of the healing agent – healing from 7 to 14 days showed a decrease in sorptivity from 573% to 196% and 792% to 467% for healed and control samples with tubes respectively.

Cracked control samples with and without tubes showed little variation in sorptivity and sorptivity reduction over healing time. This suggests that the presence of the tubes within the specimen has little effect on the healing. Cracked control specimens for this experimentation grew crystals within the cracks during the healing process in the water bath (see Figure 25). This is likely to have resulted in the measured sorptivities of these specimens being lower than they would have otherwise been had the only effect been the usual autogenous healing of the concrete.

Figure 25: Photograph showing crystals that grew within the cracks of control samples during the healing time within the water bath.

After 28 days healing the healed specimens had sorptivities of 159% of the uncracked control sorptivity. This is an encouraging result and shows that the crack is almost entirely closed (with the extra 59% due to mircoscopic gaps in the mineral structure into which water can be drawn by capillary action). The sorptivity of the uncracked control also reduced over time and thus, although not apparent from the figure, the healed specimens showed a sorptivity at 28 days of 46% of the sorptivity of the uncracked specimen at 14 days. Further experimentation would be required in order to determine a maximum achievable recovery using this healing agent and delivery method but the healed specimens still show a good reduction in sorptivity in comparison to unhealed specimens.

It should be noted that the lack of a straight line for the sorptivity results suggests that there are different strata of mineral that the water must permeate in order to travel up into the crack by capillary action.

4.5 Summary

The above results show that the vascular networks designed and tested in this project show good potential for use within self-healing concrete structures. As a summary the results may be tested against the "Criteria for 'robust' self-healing in concrete" described in Section 2.2.1:

1. Pervasiveness - In this method of self-healing the complexity of the vascular network embedded dictates whether the healing mechanism is ready for local activation at any time. In the above experimentation crack plane coverage of up to 63% was achieved although this may be improved by locating the network higher within the specimen and altering pump pressure. Within the confines of this experiment local activation was achieved (effectively at any time) although networks may need to be more complex in structures likely to fail in a number of different modes.

2. Stability - The network itself, being made from polymer, will be chemically stable within the matrix although there may be some worries as to the stability of the colloidal silica healing agent used over time. Further experimentation is needed to establish the stability of this method of healing over a time scale similar to the lifespan of a typical concrete structure.

3. Reliability - Reliability was dramatically improved within this project through altering the material used to manufacture the networks. This ensured that the network was sufficiently brittle to fracture consistently in the same location as the surrounding matrix. Despite this, further experimentation would be required to quantify the reliability of healing.

4. Quality - Mechanical property (strength and stiffness) recovery was low throughout the experimentation detailed above. This was primarily due to the choice of healing agent used within this project. Significantly better strength and stiffness recoveries of greater than 100% have been achieved in recent studies using cyanoacrylate adhesive healing agent although there are environmental and health hazards associated with using this type of healing agent as detailed in Section 2.3.3. Cracks were filled thoroughly by healing agent with visible crack obscurement of 99% after 14 days healing and sorptivities of 159% of an uncracked control specimen achieved after 28 days healing.

5. Repeatability - Repeatability of healing is a key advantage of vascular networks over other self-healing mechanisms. Although this project was unable to achieve consistent healing over multiple cycles it did show that this should be achievable as long as the healing agent does not solidify within the network or is cleared from the network after healing.

6. Economics - A full cost analysis of this particular method of self-healing in concrete is yet to be carried out. However, as 3D printing technology develops, the cost of manufacturing customizable networks to be embedded within concrete structures is likely to drop substantially. This development is likely to make the system far more financially viable as the cost is then dominated by the labour required to install the networks. This cost would not be significantly larger than the cost associated with installing complex reinforcement within structures.

These results have shown that biomimetic vascular networks show considerable promise for the autonomous self-healing of concrete. However further research and development must prove they are a viable option over autogenic or microcapsule based healing. The findings of this experimentation have highlighted directions for further research, which will be explored in the next section.

5 Conclusion

5.1 Key Findings

There are both economic and environmental advantages to making structures within the built environment more sustainable. Self-healing concrete represents an exciting route to achieving this goal.

State of the art research has identified the use of biomimetic vascular networks as a means creating self-healing concrete. These studies were used to provide a basis for preliminary investigations into the functionality of this system of self-healing.

The use of a closed circulatory system to transfer healing fluid to the damage site was proposed. It was shown through preliminary investigations that a peristaltic pump was sufficient to provide healing agent reliably to the crack plane.

Healing agent release was initially unreliable due to networks fracturing in a different location to the surrounding mortar matrix. It was postulated that this was due to the PLA networks not being brittle enough. Thus an investigation into different network manufacturing materials was undertaken. ABS networks were found to be more brittle. They reliably fractured in the same location, and simultaneously with, the surrounding matrix.

Microscopy techniques demonstrated that the bottom faces of cracks within specimens were filled far faster in healed samples than controls. Cracks in healed samples with three horizontal tubes were found to be 96% obscured after 10 days healing and all fully obscured after 28 days.

Sorptivity testing supported these results. This testing showed that specimens with networks embedded and healing agent delivered to the damage site healed significantly better than controls. After 28 days healing, healed samples showed a sorptivity of 159% of the sorptivity of an uncracked control whilst the equivalent value for cracked controls was 401%. These results showed that the healed specimens achieved good durability recovery.

The design of the network was found to have an effect on the specimen's recovery of mechanical and durability properties. Specimens with more tubes at the crack plane allowed for a more complete healing agent coverage of the crack face. Maximum crack face coverage of 63% was achieved in specimens with three horizontal healing agent delivery tubes. This increase in crack face coverage was found to be positively correlated with the recovery of specimen properties.

5.2 Improvements

Reliable cracking and healing agent leakage was achieved, effectively filling the crack with healing agent after initial cracking. Healing over multiple cycles was not investigated as solidified healing agent blocked the majority of networks after the initial 28 days healing.

Crack filling has been achieved with other systems but the key advantage of biomimetic vascular networks over other techniques of self-healing is they have the potential to provide healing over multiple cycles. As a result improvements to the above system and experimental method would be well advised to focus on achieving reliable healing agent release over several damage events. This might be obtained through the use of a different circulation regime throughout the healing cycle. For example, the peristaltic pump could be used to circulate fluid every few days during healing to try and prevent solidification of the healing agent. Another method might be to pump air, or a cleaning fluid, through the system to attempt to clear it of healing agent.

This project has looked to biological systems for inspiration. It may be of use to conduct an investigation into how biological systems heal themselves whilst preventing the blocking of the vascular network providing the healing fluid.

Improvements to this system might also involve the incorporation of a damage sensing component that can trigger the activation of the pump and control the pump's operation other time to prevent network blockage and provide reliable healing. This would upgrade the proposed system from a smart structure to an intelligent structure.

The recovery of mechanical properties, namely strength and stiffness, needs to be greatly increased in order to make this method of self-healing viable. Ideally load and stiffness recoveries will be consistently equal to, or greater than, 100%. This improvement may be made through the use of a different healing agent such as cyanoacrylate glue although this change brings with it problems of pressurising an irritant liquid within the network.

5.3 Recommendations for Future Work

Results from this experimentation have allowed various conclusions to be drawn that are detailed above. They have also highlighted opportunities for further investigation.

Some avenues for future exploration are detailed below. They are split into short term projects that may be investigated within a year and long term projects that may require more time.

5.3.1 Short term projects

- Investigation into different pumping regimes - Variation of pumping pressure and timing during the damage and healing process may have a profound effect on the quality and reliability of healing. Increased pumping pressure may allow for increased penetration of healing agent into the crack. Circulation of the healing agent during the healing process may prevent blockage of the network.

- Design of vascular networks to heal other failure modes - Tensile cracking, tested here, is only one possible mode in which cementitious materials may fail. The networks designed here would not necessarily fracture under other failure modes such as shear and shrinkage cracking. The ultimate aim would be to design a network that would reliably rupture under any failure mode.

- Use of a crack closure system to apply pressure to the crack face whilst healing - Applying pressure to either side of the specimen, thus forcing the two crack faces together, has been shown to improve the quality of healing [15]. This may have a profound effect on the quality of healing achieved with these networks.

- Design and embed networks in larger members - The ultimate goal of research in this field is to establish a self-healing technique suitable for use in concrete structures. As a result it would be of benefit to test specimens of a size more likely to be used in industry such as those used by Pang et al. [29].

- Investigate the use of different healing agents - Different healing agents may allow for far better recovery of mechanical properties as detailed in various studies [10], [46]. Consideration of the health and safety risks of pressurising a liquid irritant would be required.

5.3.2 Longer term projects

- Computational modelling of damage and healing in vascular systems - Some studies have aimed to develop a computational approach to modelling self-healing. Nguyen has investigated finite element analysis of progressive damage in self-healing composites [47]. Joseph has achieved some success in capturing fracture patterns and recovery with lattice modelling methods [48]. If these were combined and expanded with analytical work from other studies then a computation model for self-healing using vascular networks may be able to be developed [49], [50].

- Investigate novel methods of visualizing the healing process - Primary healing action occurs within the cracks and hence may not easily be observed by conventional methods. Research is currently looking into the use of computed tomography (CT) scanning as a way of viewing internal healing within specimens [51]. It may be beneficial to explore the use of methods such as this to attempt to monitor the network flow and release of healing agent in real time.

Self-healing cementitious materials offer a solution to the large environmental and economic costs of traditional concrete structures.

Almost all biological systems contain vascular networks through which a functional fluid is circulated. This observation provides the inspiration for vascular networks for self-healing in concrete. Progress has been made in investigating the viability of 3D printed networks. In the short term it is hoped that further progress will be made towards producing reliable and effective healing with these networks. In the long term traditional concrete structures could become a thing of the past with new, sustainable, intelligent structures coming to dominate our civil infrastructure.

Acknowledgements

I would like to thank Prof. Abir Al-Tabbaa for her supervision of the project, her guidance and her knowledge of the literature. I would also like to thank Dr Antonis Kanellopoulos for taking over the role for the last two months and for his patience, encouragement, advice and suggestions for experimental work throughout the process.

The Division D technicians Chris Knight, Phil McLaren and Martin Touhey were invaluable in providing help with experimentation and I am grateful to them for their advice and help with practical work.

References

[1] J. M. Crow, “The concrete conundrum,” *Chemistry World*, pp. 62–66, Mar-2008.

[2] K. Van Breugel, “Is There a Market for Self-healing Cement-based materials?,” in *Proceedings of the First International Conference on Self Healing Materials*, 2007, pp. 1–9.

[3] H. G. van Oss, “Background Facts and Issues Concerning Cement and Cement Data,” *U.S. Geol. Surv.*, p. 88, 2005.

[4] M. De Rooij, E. Schlangen, K. van Tittleboom, and N. de Belie, *Self-Healing Phenomena in Cement-Based Materials*. State-of-the-Art Report of RILEM Technical Committee 221-SHC : Self-Healing Phenomena, 2013.

[5] J. Woudhuysen and I. Abley, *Why is construction so backward?*, 1st ed. John Wiley & Sons, 2004.

[6] V. C. Li and E. Herbert, “Robust Self-Healing Concrete for Sustainable Infrastructure,” *J. Adv. Concr. Technol.*, vol. 10, no. 6, pp. 207–218, 2012.

[7] DEFRA, “Joint UK-Sweden Initiative on Sustainable Construction,” 2005.

[8] S. van der Zwaag, “An Introduction to Material Design Principles: Damage Prevention versus Damage Management,” in *Self Healing Materials SE - 1*, vol. 100, S. van der Zwaag, Ed. Springer Netherlands, 2007, pp. 1–18.

[9] E. Schlangen, H. Jonkers, S. Qian, and A. Garcia, “Recent advances on self healing of concrete,” in *Proceedings of Fracture Mechanics of Concrete and Concrete Structures*, 2010, (B. H. Oh).

[10] M. Wu, B. Johannesson, and M. Geiker, “A review: Self-healing in cementitious materials and engineered cementitious composite as a self-healing material,” *Constr. Build. Mater.*, vol. 28, no. 1, pp. 571–583, 2012.

[11] E. Schlangen and C. Joseph, “Self-Healing Processes in Concrete,” in *Self-Healing Materials*, Wiley-VCH Verlag GmbH & Co. KGaA, 2009, pp. 141–182.

[12] M. R. de Rooij, E. Schlangen, and C. Joseph, “Introduction,” in *Self-Healing Phenomena in Cement-Based Materials SE - 1*, vol. 11, M. de Rooij, K. Van Tittelboom, N. De Belie, and E. Schlangen, Eds. Springer Netherlands, 2013, pp. 1–17.

[13] S. Igarashi, M. Kunieda, and T. Nishiwaki, “Research Activity of JCI technical committee TC-075B: Autogenous healing in cementitious materials,” *Proc. 4th Int. Conf. Constr. Mater. Performance, Innov. Struct. Implic. ConMat*, pp. 89–96, 2009.

[14] British Standards Institution, *Eurocode 2: design of concrete structures: British standard*. London UK, 2008.

[15] V. Li and E.-H. Yang, “Self Healing in Concrete Materials,” in *Self Healing Materials SE - 8*, vol. 100, S. van der Zwaag, Ed. Springer Netherlands, 2007, pp. 161–193.

[16] N. Hearn and C. T. Morley, “Self-sealing property of concrete - Experimental evidence,” *Mater. Struct.*, vol. 30, no. 7, pp. 404–411, 1997.

[17] C. Edvardsen, “Water permeability and autogeneous healing of cracks in concrete,” *ACI Mater. J.*, vol. 96, no. 96, pp. 448–454, 1999.

[18] B. Hilloulin, K. Van Tittelboom, E. Gruyaert, N. De Belie, and A. Loukili, “Design of polymeric capsules for self-healing concrete,” *Cem. Concr. Compos.*, vol. 55, pp. 298–307, 2015.

[19] K. L. Bachmeier, A. E. Williams, J. R. Warmington, and S. S. Bang, “Urease activity in microbiologically-induced calcite precipitation,” *J. Biotechnol.*, vol. 93, no. 2, pp. 171–181, Feb. 2002.

[20] W. De Muynck, N. De Belie, and W. Verstraete, “Microbial carbonate precipitation in construction materials: A review,” *Ecol. Eng.*, vol. 36, no. 2, pp. 118–136, 2010.

[21] H. Mihashi, Y. Kaneko, T. Nishiwaki, and K. Otsuka, “Fundamental study on development of intelligent concrete characterized by self-healing capability for strength.,” *Trans. Japan Concr. Inst.*, vol. 22, no. 2, pp. 441–450, 2000.

[22] M. Nosonovsky and P. Rohatgi, “Self-Healing Materials,” in *Biomimetics in Materials Science SE - 1*, vol. 152, Springer New York, 2012, pp. 1–22.

[23] S. van der Zwaag, N. H. van Dijk, H. M. Jonkers, S. D. Mookhoek, and W. G. Sloof, “Self-healing behaviour in man-made engineering materials: bioinspired but taking into account their intrinsic character.,” *Philos. Trans. A. Math. Phys. Eng. Sci.*, vol. 367, no. 1894, pp. 1689–1704, 2009.

[24] C. Dry, “Smart multiphase composite materials that repair themselves by a release of liquids that become solids,” *… Smart Struct. Mater.*, vol. 2189, pp. 62–70, 1994.

[25] C. Dry, “Matrix cracking repair and filling using active and passive modes for smart timed release of chemicals from fibers into cement matrices,” *Smart Mater. Struct.*, vol. 3, no. 2, pp. 118–123, 1999.

[26] C. M. Dry, “Smart earthquake-resistant materials: using time-released adhesives for damping, stiffening, and deflection control,” 1996, vol. 2779, pp. 958–967.

[27] C. Dry and W. McMillan, “Three-part methylmethacrylate adhesive system as an internal delivery system for smart responsive concrete,” *Smart Mater. Struct.*, vol. 5, no. 3, pp. 297–300, 1999.

[28] T. D. P. Thao, T. J. S. Johnson, Q. S. Tong, and P. S. Dai, “Implementation of self-healing in concrete – Proof of concept,” *IES J. Part A Civ. Struct. Eng.*, vol. 2, no. 2, pp. 116–125, Apr. 2009.

[29] D. S. Pang, T. D. P. Thao, and S. . Quek, “Self-healing concrete structural elements,” in *3rd International Conference on Self-healing Materials*, Bath, UK, 2011, pp. 322–323.

[30] C. Joseph, A. D. Jefferson, B. Isaacs, R. J. Lark, and D. R. Gardner, “Experimental investigation of adhesive-based self-healing of cementitious materials,” no. 11, pp. 831–843, 2010.

[31] C. Dry and M. Corsaw, “A comparison of bending strength between adhesive and steel reinforced concrete with steel only reinforced concrete,” *Cem. Concr. Res.*, vol. 33, no. 11, pp. 1723–1727, Nov. 2003.

[32] T. Nishiwaki, H. Mihashi, B.-K. Jang, and K. Miura, “Development of Self-Healing System for Concrete with Selective Heating around Crack,” *J. Adv. Concr. Technol.*, vol. 4, no. 2, pp. 267–275, 2006.

[33] V. C. Li, Y. M. Lim, and Y.-W. Chan, “Feasibility study of a passive smart self-healing cementitious composite,” *Compos. Part B Eng.*, vol. 29, no. 6, pp. 819–827, 1998.

[34] S. R. White, N. R. Sottos, P. H. Geubelle, J. S. Moore, M. R. Kessler, S. R. Sriram, E. N. Brown, and S. Viswanathan, “Autonomic healing of polymer composites.,” *Nature*, vol. 409, no. 6822, pp. 794–797, 2001.

[35] C. Dry, “Procedures Developed for Self-Repair of Polymeric Matrix Composite Materials,” *Compos. Struct.*, vol. 35, pp. 263–269, 1996.

[36] S. M. Bleay, C. B. Loader, V. J. Hawyes, L. Humberstone, and P. T. Curtis, “A smart repair system for polymer matrix composites,” *Compos. - Part A Appl. Sci. Manuf.*, vol. 32, no. 12, pp. 1767–1776, 2001.

[37] J. W. C. Pang and I. P. Bond, “‘Bleeding composites’—damage detection and self-repair using a biomimetic approach,” *Compos. Part A Appl. Sci. Manuf.*, vol. 36, no. 2, pp. 183–188, Feb. 2005.

[38] J. W. C. Pang and I. P. Bond, “A hollow fibre reinforced polymer composite encompassing self-healing and enhanced damage visibility,” *Compos. Sci. Technol.*, vol. 65, no. 11, pp. 1791–1799, 2005.

[39] K. S. Toohey, N. R. Sottos, J. a. Lewis, J. S. Moore, and S. R. White, “Self-healing materials with microvascular networks,” *Nat. Mater.*, vol. 6, no. 8, pp. 581–585, 2007.

[40] C. J. Hansen, W. Wu, K. S. Toohey, N. R. Sottos, S. R. White, and J. a. Lewis, “Self-healing materials with interpenetrating microvascular networks,” *Adv. Mater.*, vol. 21, no. 41, pp. 4143–4147, 2009.

[41] K. S. Toohey, C. J. Hansen, J. A. Lewis, S. R. White, and N. R. Sottos, “Delivery of two-part self-healing chemistry via microvascular networks,” *Adv. Funct. Mater.*, vol. 19, no. 9, pp. 1399–1405, 2009.

[42] C. Kimber, “Biomimetic Vascular Networks for Self-Healing Concrete.” CUED, 2014.

[43] "CubeX Technical Specifications." [Online]. Available: http://www.midwich.com/media/pdf/Q413-3640-CubeX_3D_Printer_technical_specification.pdf. [Accessed: 20-May-2015].

[44] J. Pitroda and D. Umrigar, "Evaluation of Sorptivity and Water Absorption of Concrete with Partial Replacement of Cement by Thermal Industry Waste (Fly Ash)," *Int. J. Eng. Innov. Technol.*, vol. 2, no. 7, pp. 245–249, 2013.

[45] J. Kropp, "RILEM TC 116-PCD Permeability of Concrete as a Criterion of its Durability.pdf," vol. 32, no. April, pp. 174–179, 1999.

[46] N. De Belie and K. Van Tittelboom, "Self-healing concrete : suitability of different healing agents," *International Journal of 3R's*, vol. 1, no. 1. pp. 12–21, 2010.

[47] T. Nguyen and A. Orifici, "Structural assessment of microvascular self-healing laminates using progressive damage finite element analysis," *Compos. - Part A Appl. Sci. Manuf.*, vol. 43, no. 11, pp. 1886–1894, 2012.

[48] C. Joseph, "Experimental and numerical study of the fracture and self-healing of cementitious materials," Cardiff University, UK, 2008.

[49] H. R. Williams, R. S. Trask, A. C. Knights, E. R. Williams, and I. P. Bond, "Biomimetic reliability strategies for self-healing vascular networks in engineering materials," *J. R. Soc. Interface*, vol. 5, no. 24, pp. 735–747, Jul. 2008.

[50] H. R. Williams, R. S. Trask, P. M. Weaver, and I. P. Bond, "Minimum mass vascular networks in multifunctional materials," *J. R. Soc. Interface*, vol. 5, no. 18, pp. 55–65, Jan. 2008.

[51] K. Van Tittelboom, D. Van Loo, N. De Belie, and P. Jacobs, "Evaluation of the Efficiency of Self-Healing in Concrete by Means of μ-CT," in *Advances in Computed Tomography for Geomaterials*, John Wiley & Sons, Inc., 2013, pp. 132–139.

[52] C. M. Dry, "Three designs for the internal release of sealants, adhesives, and waterproofing chemicals into concrete to reduce permeability," *Cem. Concr. Res.*, vol. 30, no. 12, pp. 1969–1977, 2000.

[53] C. A. Harper and A. Baker, *Modern Plastics Handbook*. New York: McGraw-Hill, 2000.

Appendix

Appendix A: Risk Assessment Retrospective

At the start of the project a risk assessment, identifying chemical, mechanical and office-based hazards, was submitted to the Health and Safety Office. This aided in formulating a safe system of work.

Various safety measures were taken throughout the project. A dust mask was worn when handling cement powder. Gloves were worn when handling chemicals and steel capped boots were worn at all times in the workshop and when handling specimens.

The initial risk assessment effectively identified the hazards present during the project and no issues were reported.

Appendix B: Full Tabulated Results from Microscopy Examination of Specimens

Specimen No.	Initial Crack Width / mm	Percentage of Crack Area Filled		
		10 days	20 days	28 days
1T.1	0.89	26.1%	31.3%	45.3%
1T.2	0.97	25.4%	34.5%	46.2%
1T.3	1.23	26.8%	26.3%	43.3%
1T.CONTROL	1.18	26.7%	33.2%	45.2%
2T.1	0.79	100.0%	100.0%	100.0%
2T.2	0.91	93.9%	100.0%	100.0%
2T.3	0.74	43.4%	59.7%	72.5%
2T.CONTROL	0.86	22.9%	32.1%	47.7%
3T.1	0.81	91.1%	98.9%	100.0%
3T.2	1.01	95.8%	100.0%	100.0%
3T.3	0.71	100.0%	100.0%	100.0%
3T.CONTROL	1.05	24.0%	29.1%	42.8%

Appendix C: Full Tabulated Results from Sorptivity Experimentation

This table shows the sorptivities of all specimens tested. In Figure 24 (within the main body of the report) values are listed as percentages of the sorptivity of the "Uncracked Control".

	SORPTIVITY / ($g/mm^{-2}s^{-0.5}$)							
	Specimen 1	Specimen 2	Specimen 3	Specimen 4	Average of Test Specimens	Control with Network	Control without Network	Uncracked Control
7 DAYS	0.322	0.348	0.374	0.404	0.362	0.501	0.490	0.063
14 DAYS	0.113	0.099	0.035	0.106	0.088	0.210	0.190	0.045
28 DAYS	0.022	0.021	0.020	0.021	0.021	0.053	0.060	0.013